A Dissertation

for the Degree of Masters of Sciences

Enhancement of immunogenicity through conjugation of complement fragment C4d to porcine epidemic diarrhea virus surface protein antigen, S0

보체 절편 C4d 의 돼지유행성설사 바이러스 표면 항원 S0 에 결합을 통한 면역증진

February 2019

By

Young-Saeng Kim Cho

Department of Agricultural Biotechnology

Graduate School

Seoul National University

농 학 석 사 학 위 논 문

Enhancement of immunogenicity through conjugation of complement fragment C4d to porcine epidemic diarrhea virus surface protein antigen, S0

보체 절편 **C4d** 의 돼지유행성설사 바이러스 표면 항원 **S0** 에

결합을 통한 면역증진

지도교수 최 윤 재

이 논문을 농학 석사 학위 논문으로 제출함.

2019 년 1 월

서울대학교 대학원

농생명공학부 동물생명공학전공

조영생

조영생의 석사학위논문을 인준함.

2019 년 1 월

위 원 장 윤 철 희 (인)

부 위 원 장 최 윤 재 (인)

위 원 강 상 기 (인)

Summary

The current landscape for vaccines is colored with concerns about the safety of vaccines in the wake of live attenuated or inactivated vaccines. From these concerns, subunit vaccines have risen into the next hot topic for vaccine production. The main advantage of a subunit vaccine is its inherent characteristic of consisting of the antigen-neutralizing subunit of the whole virus, being an inherently safer alternative to other types of vaccines. However, the biggest disadvantage a subunit vaccine must overcome is its low immunogenicity compared to live attenuated vaccines. In order to increase the immunogenicity of the subunit vaccine consisting of the S0 spike protein from PEDV's (Porcine Epidemic Diarrhea Virus) coronavirus, complement fragment C4d was used as a fusion adjuvant.

Cloning by using isocaudomers was successful and was confirmed by fragment size distribution through agarose gel electrophoresis and Sanger sequencing. It is important to express recombinant proteins in a soluble way, so three factors were optimized to increase solubility. The first factor was a chaperone, the second was optical density, and the third was IPTG (isopropyl β-D-1-thiogalactopyranoside) concentration. After optimization experiments, it was determined that trigger factor chaperone must be co-expressed with target proteins. In addition, the optimal optical density for inducing proteins is A_{600} = 0.6, which is during the mid-log phase of growth, using 0.1 mM IPTG. The new, optimized protocol was used for expressing the recombinant proteins S0, S0-mC4d1, S0-mC4d2, and

mC4d in a large scale 500 mL flask. The proteins were purified using Ni-NTA (Nickel-nitrilotriacetic acid) resin and dialyzed in PBS (phosphate buffered saline) before being concentrated down.

After finding the concentration of the proteins, 6 groups of mice were immunized using the same molar concentration of proteins. The groups were, PBS control, S0 control, the two fusion protein groups, and two mixture groups. After immunization, serum and spleens were taken from the mice and used for ELISA (enzyme-linked immunosorbent assay) and ELISpot (enzyme-linked immunospot), respectively. ELISA shows that end point titers of IgG increased significant in S0-mC4d2 and two mixture groups after 4 weeks and in all mC4d treatment groups after 6 weeks. ELISpot shows the presence of mC4d-specific Th2 cells in the two fusion protein groups but not in the S0 or the mixture groups.

In conclusion, recombinant proteins were produced well with relatively high yield and purity and immunization results show that S0-mC4d1 and S0-mC4d2 increases humoral immunity through C4d-specific auto-reactive Th2 cells.

Keywords: Porcine Epidemic Diarrhea. Porcine Epidemic Diarrhea Virus. Adjuvant. Subunit vaccine. C4d. Fusion Adjuvant. Spike protein. Recombinant protein. Optimization. Solubility

Student number: 2016-27810

Contents

List of Tables and Figures

Tables

Figures

List of Abbreviations

A_{600} = Optical density at a wavelength of 600 nm

ACK lysis buffer: Ammonium-Chloride-Potassium lysis buffer

APC: Antigen presenting cell

BLAST: Basic Local Alignment Search Tool

BSA: Bovine serum albumin

CFA: Complete Freund's Adjuvant

DNA: Deoxyribonucleic acid

ECL: Enhance chemiluminescence

ELISA: Enzyme-linked immunosorbent assay

ELISpot: Enzyme-linked immunospot assay

FBS: Fetal bovine serum

Flagellin-EGFP: Flagellin enhanced fluorescent protein

HRP: Horseradish peroxidase

IB: Inclusion bodies

IEDB: Immune Epitope Database

IFA: Incomplete Freund's Adjuvant

IL-18: Interleukin-18

IMD: Imidazole

IPTG: Isopropyl β-D-1-thiogalactopyranoside

LB: Lysogeny broth

MBL: Mannose binding lectin

mC4d: Mouse C4d

MHC: Major histocompatibility complex

Ni-NTA: Nickel-nitrilotriacetic acid

pAPN: Porcine aminopeptidase N

PBS: Phosphate Buffer Saline

PED: Porcine Epidemic Diarrhea

PEDV: Porcine Epidemic Diarrhea Virus

P/S: Penicillin/Streptomycin

RNA: Ribonucleic acid

ssRNA: single strand RNA

RT: Room temperature

RPMI 1640: Roswell Park Memorial Institute medium

SDS-PAGE: Sodium dodecyl sulfate – polyacrylamide gel electrophoresis

SPF: Specific-pathogen-free

TBST: Tris Buffered Saline with Tween 20

tig: Trigger factor chaperone

I. Introduction

Porcine epidemic diarrhea (PED) is an economically significant disease within the pig farming industry due to its devastating effects on the pork industry. PEDV is the etiological agent of PED. The disease mainly affects mostly piglets and has and can completely destroy a farmer's yield, with mortality rates of up to 100% (Sun, Cai et al. 2012). Current vaccination strategies in Korea consist of live attenuated vaccines that have been developed to vaccinate pregnant sows and protect piglets through passive immunity (Song and Park 2012). The use of vaccines based on live organisms can produce a powerful immune response and thus, a large portion of licensed vaccines fall into the live attenuated vaccine or inactivated vaccine category (Perrie, Kirby et al. 2007). In fact, most commercial PED vaccines come from attenuated live or killed viruses. These vaccines can be effective; however, safety concerns have been raised regarding their application. Antigenic variation and safety concerns make it difficult for generic commercial live attenuated or inactivated PEDV to protect animals from disease. Recombinant subunit vaccines are an alternative vaccine candidate to ameliorate this safety issue as subunit vaccines are safer, easier to produce, and more cost-effective than live attenuated vaccines.

Due to the low immunogenicity of subunit vaccines, fusion adjuvant strategy (Perrie, Mohammed et al. 2008) was deemed to be the most prudent plan of action. By fusing the adjuvant directly onto the antigen, the chance of being engulfed

together increases. C4d was the fusion adjuvant of choice. C4d's mechanism may follow that of C3d's wherein, T-cell epitopes of C4d may be presented to auto-reactive T helper cells with the ability to activate B cells that have recognized the spike protein. The end result is the differentiation of B cells into plasma cells.

In this study an *E. coli* expression system was used to produce recombinant proteins that consist of S0 fused with tandem repeats of mC4d linked together with glycine-serine linkers. In the first part of this study recombinant protein plasmids were constructed by using restriction enzymes to cut the vector, pET28a (+), and the insert, mC4d, and ligate them together. Then, classical cloning techniques were utilized to produce the final products as recombinant plasmids. In the next part, the recombinant plasmids were extracted from their cloning hosts and transformed expression hosts with the recombinant plasmids. The bioreactor most commonly used to produce recombinant protein-based subunit vaccines are *E. coli* due to their relatively high production yield. However, expression of recombinant proteins in *E. coli* often results in the formation of insoluble aggregates known as inclusion bodies (IB). Chaperone co-expression strategies have been proposed to facilitate soluble expression of recombinant proteins. In this section of the study, the focus was to optimize the production of the proteins by utilizing a protein chaperone and adjusting physiological aspects of the protein production procedure. Finally, the effects on humoral and cellular immunity of the recombinant proteins were evaluated in immunized mice through indirect ELISA and ELISPOT assay, respectively.

II. Review of Literature

1. Porcine Epidemic Diarrhea Virus

1) Overview of Porcine Epidemic Diarrhea

Porcine epidemic diarrhea is an economically devastating viral enteritis in pigs. The causative agent is PEDV (Song, Moon et al. 2015). Characterized mainly by watery diarrhea and vomiting, the severe water loss eventually leads to dehydration, depression, and death (Lee 2015). PEDV infects pigs of all stages of development and the most important age group is in neonatal piglets as the dehydration and diarrhea commonly leads to death rates of 80% to 100% (Sun, Cai et al. 2012). PEDV's rapid spreading across various countries of the world not only brings illness and loss of pig lives, but also poses a threat to the economic ventures of the swing farming industry and public health as a whole (Huang, Dickerman et al. 2013).

First observed in 1971 as an unrecognized enteric disease in pigs, the etiological agent that was identified as the main cause was the PEDV prototype strain CV777 (Huang, Dickerman et al. 2013). The disease spread across Europe affecting pigs of all ages until the 1990s when PED's effects subsided in Europe but had since spread across Asia (Lee 2015), jumping continents. Since its emergence in South Korea in 1992, PEDV has been a constant occurrence each year until 2010 (Lee and Lee 2014). From the 1980s to present day, PED has caused higher rates of

mortality than when previously encountered in European countries becoming an endemic in Asian pig farming countries (KUSANAGI, KUWAHARA et al. 1992, Song and Park 2012). In 2013, PEDV suddenly experienced a resurgence when the first case of PEDV was recorded in the United States and quickly spread across North America. Recent strains of PEDV in South Korea appear to be the most genetically like the strains of PEDV from the 2013 outbreak in the United States marking 2013 as a landmark year for PEDV research (Lee and Lee 2014, Lin, Chung et al. 2014).

2) Porcine Epidemic Diarrhea Virus

The etiological agent of PED is the enveloped RNA virus porcine epidemic diarrhea virus (Lin, Chung et al. 2014). The taxonomical classification of PEDV is of the genus *Alphacoronavirus* and within the *Coronaviridae* family. The genome protein size is 28 kb long and contains at least 7 open reading frames, 4 of which encode for the structural proteins including the glycosylated spike protein (S), nucleocapsid protein (N), membrane protein (M), and the envelope protein (E) (Lee 2015).

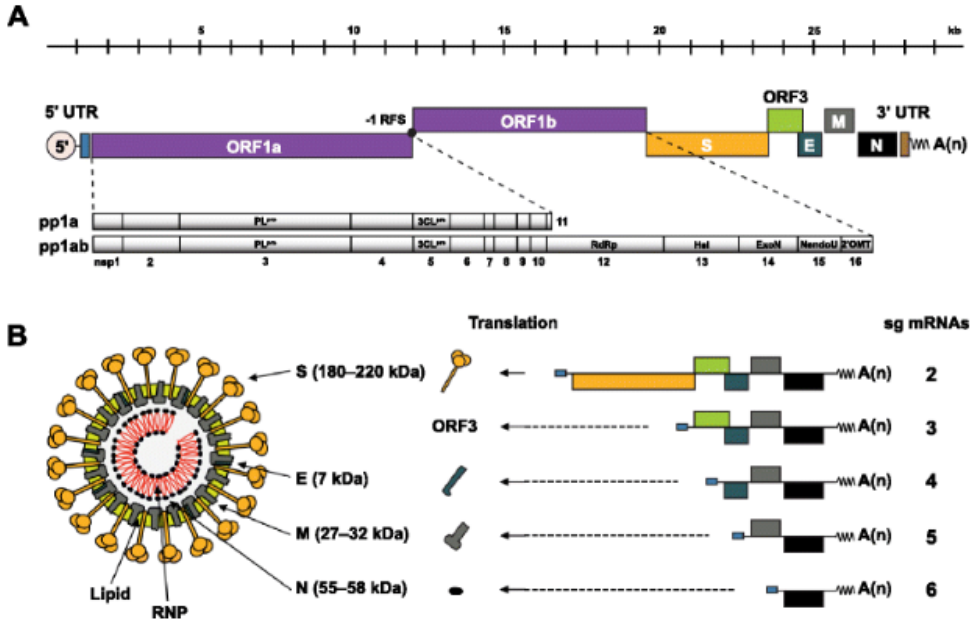

Figure 1. Genome organization and the structure of PEDV. (A) Structure of PEDV genomic RNA (B) Model of PEDV structure (Lee 2015)

As noted above, the structural proteins of PEDV consist of the S, E, M, and N proteins. The spike (S) protein interacts with the pAPN (porcine aminopeptidase N) receptor during virus entry and is often used to stimulate neutralizing antibodies in the host. For example, the N-terminal domain of the S1 domain of the spike protein has been of interest. The reason for this is because some have reported that the N-terminal domain has some inactions with a sugar co-receptor, Neu5Ac, which can help PEDV bind to the enterocytes of pigs (Piao, Lee et al. 2016). Due to the antigenicity of the spike protein, it is considered as a main player in developing a defense against PED (Oh, Song et al. 2003, Li, Li et al. 2017).

Typically, PEDV strains are categorized into either S-INDEL or non-INDEL strains. By studying the phylogenic differences in the spike (S) gene of PEDV, researchers found that there are high amounts of differences between strains (Masuda, Murakami et al. 2015). Strains with either insertions or deletions, which indicate overall variance, are considered S-INDEL (Wang, Guo et al. 2016) while strains without insertions or deletions in the S gene are called non-INDEL. S-INDEL and non-INDEL strains are also different from one another as they also can have different amounts of danger to the pigs. As antibodies reactive against S0 from one strain will have an effect against S0 from other non-INDEL strains (Li, Li et al. 2017), S0 was selected for as the subunit candidate in this study. In addition, non-INDEL strains, which S0 has cross-reactive activity over, are considered to be more dangerous than their S-INDEL

counterparts, consist of the strains in current circulation (Jarvis, Lam et al. 2016).

The spike protein contains a wide variety of domains with each domain having their own function. It was also discovered that each domain is unique enough that antibodies that bind to one domain may not bind to a different domain within the same spike protein. Despite this, monoclonal antibodies that bind to a specific domain may bind to the same domain of a different strain as long as they are both S-INDEL or both non-INDEL (Li, Li et al. 2017).

3) Infection of the host cell

Like many animal viruses, PEDV has the ability to enter animal cells and "hijack" the cell's machinery in order to replicate and proliferate, greatly increasing its numbers after infection of the host. For this reason, PEDV is an ssRNA (single strand RNA) virus. Due to the restricted tissue tropism of PEDV, the virus seems to replicate with the most efficiency in porcine intestinal villous enterocytes. The targeted cellular receptor for PEDV's spike protein is the pAPN receptor which exists on the surface of porcine enterocytes (Nam and Lee 2010). As seen in figure 2, PEDV infects the host cell after its spike protein binds to pAPN. Once the virus has been internalized, the viral genome is released into the cytosol for genome replication and hijacking is complete (Lee 2015).

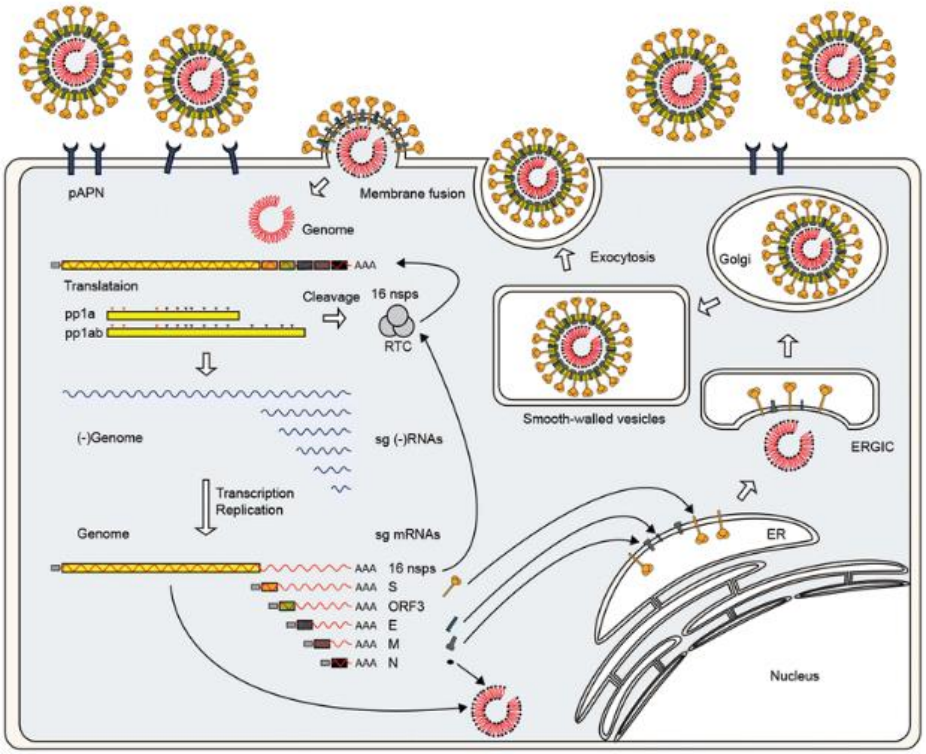

Figure 2. PEDV replication cycle and infection route via interaction of spike protein with pAPN (Lee 2015).

4) Porcine Epidemic Diarrhea Virus vaccines

In countries where PED is considered an endemic, vaccination is the best plan of action in order to contain and prevent any additional damage caused by the disease. The majority of commercially available PED vaccines fall into the category of inactivated or attenuated vaccines. (Song et al 2007). A Vero cell-attenuated PEDV PV-5 vaccine was developed first in Japan and has also become available in South Korea (Lee, 2015). Additionally, there are other cell-attenuated strains that originated from the field known as PEDV SM-98-1 and DR-13 which are used in Korean mainly (Lee, 2015). While these vaccines have staying power due to their current market use along with positive results in testing conditions, their overall effectiveness and concerns with the well-being and safety of the animals provides an outlet for the exploration of different options, especially in different types of vaccines. In addition, the efficacy and safety of commercial PEDV vaccines used in Korea has been called into question. It seems that immunity from strains that were previously considered to be endemic fail to produce cross-protection to recent PEDV strains. This may be due to recent Korean PEDV field isolates differing genetically from vaccine strains used in Korea (Ayudhya, Assavacheep et al. 2012).

Currently, there is the development of other types of vaccines as new candidates of PED. One type of vaccine is RNA/DNA vaccines. There was a report that using the DNA of the spike protein combined with IL-18 elicited humoral and cytotoxic T cell immune responses (Suo, Ren et al. 2012). A US company, Harris Vaccine

Inc., produced an RNA vaccine (Kim, Lee et al. 2016) and in 2014, Harris Vaccine Inc., was able to attain a US Department of Agriculture license and could distribute its vaccine into use. Another type comes from a South Korean research group where they inserted the core neutralizing epitope of PEDV into tobacco plants using a tobacco-mosaic virus-based vector. This resulted in a plant-based vaccine (Kang, Kim et al. 2005). Another venture is into using recombinant protein vaccines. An attempt at a subunit vaccine using porcine kidney cells to produce the PED virus spike protein has been relatively successful at producing yields (Oh, Lee et al. 2014).

2. Complement fragment C4d

1) Overview of complement fragment C4d

Complement fragment C4d is a split product of the C4 complement protein from the innate immune system's complement system. The complement system's main role is to complement the ability of antibodies and phagocytic cells to clear microbes and damaged cells, promote inflammation, and directly attack pathogens by puncturing the pathogen's cell membrane (Janeway, Travers et al. 2005). As seen in figure 3, C4, when activated by the classical pathway, is triggered by either IgM or IgG sticking to the surface of the pathogen. After complement protein complex C1qrs binds to target-bound antibodies to cleave C4 and C2. C4b sticks to C2a to form C3 convertase. C3 convertase's main role is to continue the complement cascade cleaving C3. C3b complexes with C4bC3a to form C5

convertase which can begin the membrane attack complex which will lyse the pathogenic cell (Murata and Baldwin III 2009). Formation of C3 convertase on the surface of cells amplifies the activation of complement however, chronic amplification of C3 convertase may lead to injury to the host or lysis of bystander cells.

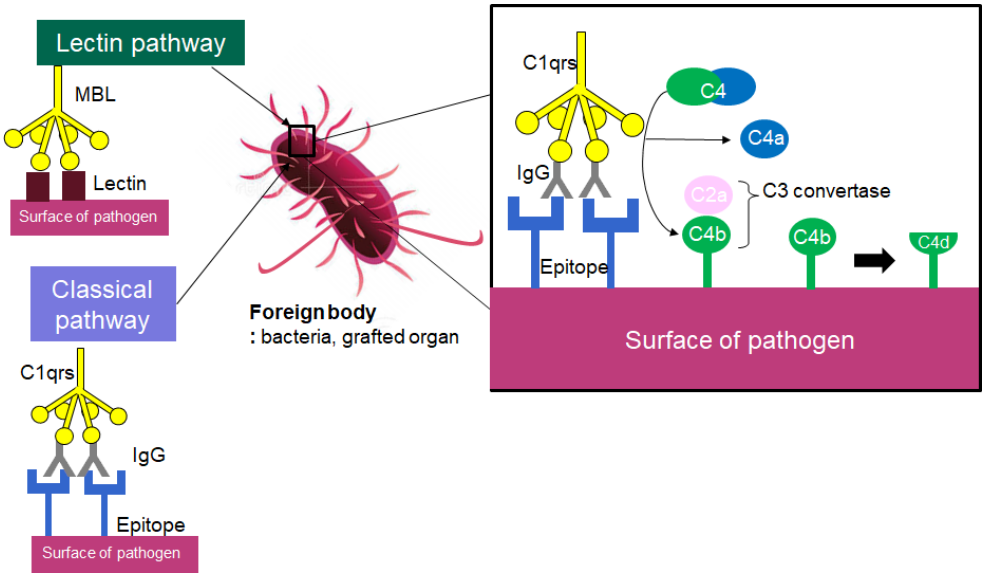

Figure 3. Formation of C4d through complement activation.

The lectin pathway is the second pathway in which C4d is also present. The lectin pathway's analog to C1q, MBL (mannose binding lectin), bind to mannose or N-acetyl glucosamine both of which are commonly found on surfaces of bacteria. After MBL binds, it complexes with C1r and C1s and the process continues like that of the classical pathway (Janeway, Travers et al. 2005).

Regardless of the pathway, C3 convertase present on the surface of cells will amplify the activation of complement. However, chronic amplification of C3 convertase may lead to injury of the host or lysis of innocent bystander cells. To put the brakes on the chronic activation of the complement cascade, C3 convertase is mediated by plasma factor I which eventually generates C4d (Platt 2002).

While bound C4d is considered an orphan ligand, it's mainstream use is as a marker of classical complement activation which can reveal antibody-based attacks against a host's cells (Feucht 2003), even after the complement system has finished the cascade. For this reason, many have used the detection of C4d to determine if the body has rejected a grafted kidney or other organ (Herzenberg, Gill et al. 2002). The exact reason for why C4d is prevalent on a rejected graft, or what its overall biological role is remains unknown (Nickeleit, Zeiler et al. 2002).

2) C3d's mechanism as an auto-reactive helper T-cell epitope donor

The proposed mechanism of C4d was extrapolated from the mechanism of the adjuvant effect from complement fragment C3d. C3d is often used as a fusion adjuvant and originally C3d was thought to be the ligand for a co-receptor on B cells that would help activate them (Carroll 2008). However, new evidence has been found that suggests that the mechanism of adjuvanticity is different. C3d has been discovered to be rich in T-cell epitopes thus creating a different, plausible narrative for how C3d acts as an adjuvant (De Groot, Ross et al. 2015). Typically, C3d would be prevalent in the wake of a complement cascade. When C3d has

adhered onto the surface of an antigen, B cells that recognize the antigen engulf both the antigen and the C3d fragment. This results in the display of both the lysed fragment of the antigen and T-cell epitopes of C3d. Pre-existing autoreactive T cells, which recognize fragments originating from complement, may recognize C3d displayed in MHC II and activate the naïve B cell immediately, resulting in an antibody producing plasma cell.

Two curiosities that arise from this situation are the characteristic of a complement fragment having an remarkable high T cell epitope content (De Groot, Ross et al. 2015) and the second oddity is the abnormal existence of C3d-specitifc auto-reactive T cells. Auto-reactive T cells, on principle, should not exist due to positive selection of naïve T cells during T cell education in the thymus (Starr, Jameson et al. 2003). These two pieces of information together suggest the existence of possible biological role of C3d along the crux of a C3d-specific autoreactive T cell axis.

Should the existence of C3d-specific autoreactive T cells be confirmed, their application opens up a new possibility of cellular immunity shown in figure 4. Hypothetically, bacteria that are linked with C3d, from the complement pathway, is phagocytized by B cells, C3d, with its inherently high content of T cell epitopes, would be fragmented and presented on the MHC-II of B cells. The MHC-II and peptide complexes can be recognized by C3d specific T cells and provide activation signals to B cells. As a characteristic of C3d is the ability to bind to a wide range of pathogens, if pathogen-specific B cells all present T cells

originating from C3d, C3d-specific T cells can still react to pathogen-specific B cells. This eliminates the need to wait for a pathogen-specific T cell to come along and find it's "perfect-match" B cell. Along with this, if C3d-specific autoreactive T cells are already primed and prepared to act, they can provide aid to naïve B cells quickly. Maturation of T cells is the rate-limiting step for antibody production (Gershon 1974) and quickening this step may speed up the entire antibody production process.

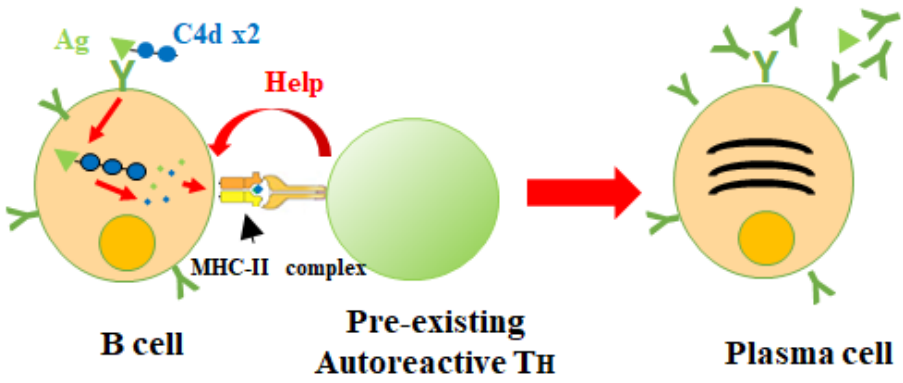

Figure 4. Mechanism of action for C4d fused with antigen of interest

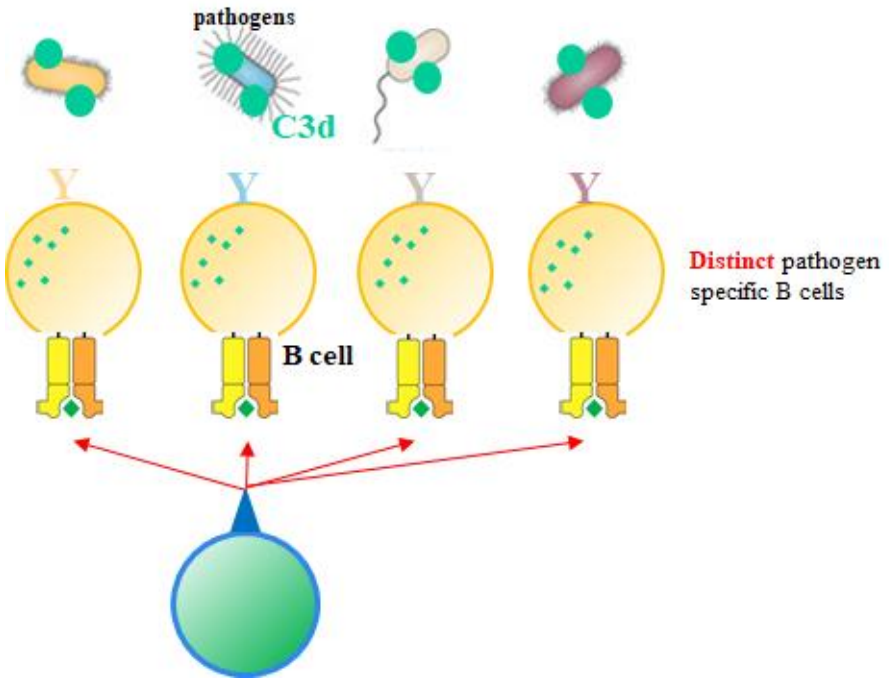

Figure 5. Proposed biological role of C3d.

3) *In silico* analysis of broad binding serum proteins

The existence of other serum proteins with similar characteristics of C3d is currently unknown. These characteristics would include the ability to attach itself to a broad range of pathogens and, perhaps more importantly, have high T cell epitope content. If both of these characteristics are satisfied, theoretically, this protein could attach itself to a pathogen and be engulfed by the pathogen-specific B cell. Presentation of the T cell epitopes within the serum protein would encourage the T cell to activate the B cell to produce antibodies. In order to find the existence of such serum proteins, *in-silico* analysis was performed.

Blood serum candidates were analyzed for T-cell epitopes using the IEDB (Immune Epitope Database) tool for MHC II (major histocompatibility complex II) binding prediction. Protein sequences for various blood serum proteins were collected using BLAST (Basic Local Alignment Search Tool), which contains a database of many DNA sequences, from the National Center for Biotechnology Information (NCBI, USA) and entered into the IEDB tool. IEDB may only make binding predictions for humans and mice and does not include the target animal, pigs, therefore human MHC II was selected along with the appropriate MHC alleles to cover about 90% of the human population (DRB1*01:01, 03:01, 07:01, 09:01, 11:01, 15:01). Despite the target animal being swine, humans were selected due to further applications possibly venturing into vaccines for humans. The tool selected every possible amino acid fragment through chopping the entire protein sequence and assigned a Z-score with lower Z-scores representing good binding ability to each of the chopped protein sequences.

The data from the tool was compiled and only fragments with Z-scores below 10 or below 5 were considered T-cell epitopes with high binding affinity for MHC II.

The rationale for selecting broadly binding serum proteins is due to the working hypothesis that autoreactive T cells have an evolutionary origin. Their ability to broadly bind to various pathogens and the existence of multiple T cell epitopes within their protein structure may be for the purpose of seeking out pathogens and creating an immune response against them.

In addition, there is an inherent advantage of having copious amounts of epitopes as increasing the probability of a B cell presenting any given epitope to a T cell in turn increases the likelihood of B cell activation. Finally, any given individual's MHC will be slightly different from another individual's due to genetic shuffling and the variability of DNA. As a result, having a diverse and broad repertoire of epitopes is an advantage because the different epitopes can activate MHC-II from different individuals. Thus, the formulated hypothesis states that broad binding serum proteins that also double as epitope donors may act in a manner similar to C3d and thus have an adjuvant-like effect for the activation of B cells through autoreactive T-helper cells.

Serum proteins were selected from common knowledge of which serum proteins bind broadly to a wide range of pathogens derived from immunology textbooks. To validate their use, an *in-silico* experiment was conducted. Protein sequences of various serum proteins were used in the IEDB database to determine their respective T-cell epitope content. The IEDB analysis tool chops up the protein sequences and measure their ability to bind with MHC-II. Fragments with high binding ability to MHC-II were given a low Z-score (below 1, 5, or 10). Using the Z-scores the database provided, the number of low Z-scores, shown in figure 7, either below 5 or below 10, for each serum protein, were graphed to produce a visualization of the amount of low Z-score fragments amongst the broad pathogen binding serum proteins.

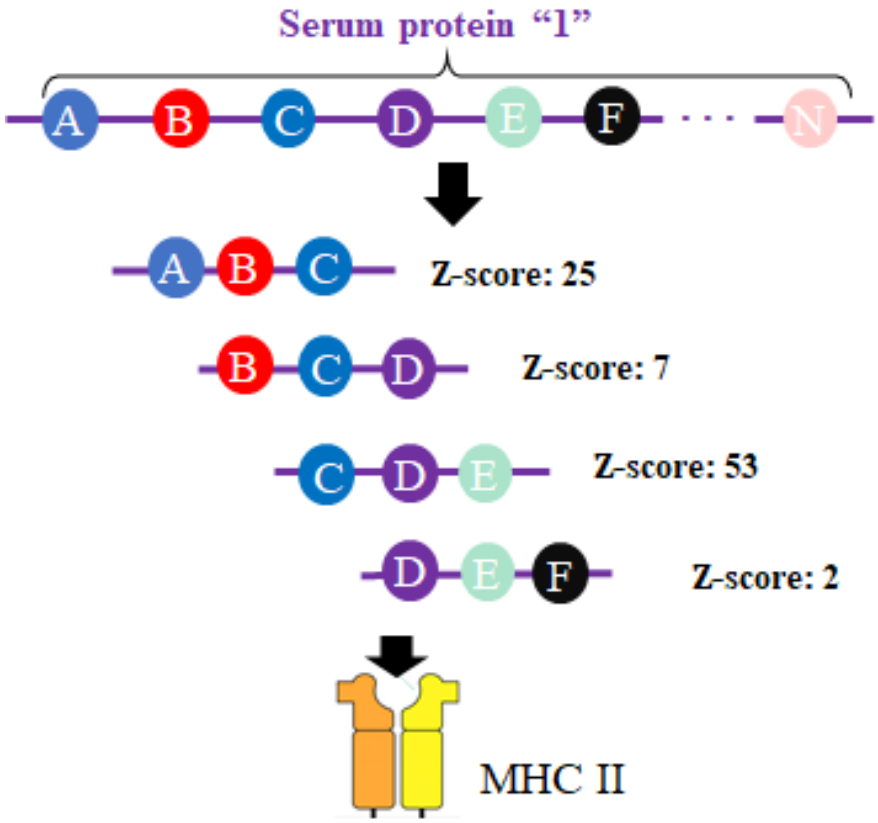

Figure 6. Premise of IEDB analysis tool.

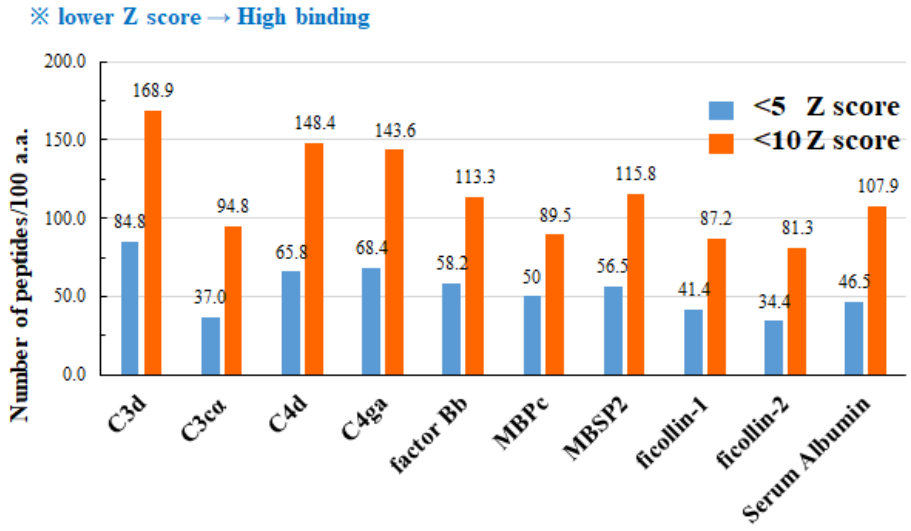

Figure 7. The number of T cell epitopes per 100 amino acids from within broad binding serum proteins.

The positive control was C3d, as it has been proven to contain a high T cell epitope content (De Groot, Ross et al. 2015) and the negative control was serum albumin. After compiling the z-score data from all the serum protein candidates, the number of fragments containing z-scores below 10 or below 5 per 100 amino acids were graphed. According to figure 7 and table 1, serum proteins containing the greatest number of low scoring peptides (z-scores below 5 or below 10) within 100 amino acids were C3d, and C4d. The negative control, serum albumin, contained 108 fragments that scored below 10 and 47 fragments per 100 amino acids that scored below 5. C4d had 149 peptides with z-scores below 10 per 100 amino acids and 66 fragments below 5 per 100 amino acids, outnumbering the number of fragments in both categories compared to the

negative control. In addition, C3d had 169 peptides with z-scores below 10 per 100 amino acids and 85 peptides with z-scores below 5 per 100 amino acids, meaning C4d's high binding peptide count is comparable with the positive control, C3d.

Table 1. Tabulated number of T cell epitopes per 100 amino acids for broad binding serum protein candidates

Z-score	C3d	C3cα	C4d	C4ga	factor Bb	MBPc	MBSP2	ficollin-1	ficollin-2	Serum Albumin
<5	84.8	37.0	65.8	68.4	58.2	50	56.5	41.4	34.4	46.5
<10	168.9	94.8	148.4	143.6	113.3	89.5	115.8	87.2	81.3	107.9

Interpretation of these data leads to the conclusion that C3d and C4d contain the greatest number of MHC-II high binding peptides, or in other words, the greatest number of T-cell epitopes.

3. Recombinant subunit vaccine

Recombinant subunit vaccines are a subtype of inactivated whole vaccines in which, only the essential epitopes of the antigen are used to inoculate the host. As such they can be an alternative vaccine type for live attenuated vaccines or traditional whole, inactivated vaccines. Various live organism-based vaccines exhibit high efficacy but can cause adverse reactions to the recipient. Generally, vaccines greatly benefit from satisfying certain criterium such as having the ability to elicit an immune response, be reasonably safe to the host, and should have wide

spread coverage, for example, a single dose administration (Perrie, Mohammed et al. 2008). Regarding the safety to the administered, subunit vaccines have several positive aspects about them that make them attractive as an alternative vaccine candidate. For the most part, subunit vaccines are widely considered to be the safer alternative to other types of vaccines because subunit vaccines do not use a virus and thus, viral replication is completely prevented. As a testament to this, many subunit vaccines are preferentially used in children and elders (Tristram, Welliver et al. 1993, Falsey and Walsh 1997). In addition to this, subunit vaccines are very high productive efficiency as the design and large-scale production process of a subunit vaccine can be quickly done and is relatively simple to complete. The completed process will yield highly-purified recombinant proteins that can induce an antigen specific immune response in the host (Coller, Clements et al. 2011).

Despite the several advantages of using subunit vaccines, there are several disadvantages as well. Namely, that subunit vaccines have low immunogenicity and low stability within the host. These issues cause high incidence of degradation and a need for multiple injections. Work arounds for this include the addition of adjuvants. It has been stated that peptides can become more immunogenic when coupled with synthesized T-cell epitopes for better binding with MHC class II (Burnette 1991).

4. Adjuvant system

1) Vaccine adjuvants

As stated above, a subunit vaccine's ability to induce an immune response is considered as low compared to other types of vaccines. Therefore, the use of adjuvants can enhance the immunogenicity of subunit vaccines (Perrie, Mohammed et al. 2008).

Adjuvants are components that may enhance or shape an antigen-specific immune response. They may be used to enhance the efficacy of weak antigens. Because subunit vaccines do not generate a large humoral response and likely no T cell response at all, multiple immunizations may be necessary to generate the desired humoral response (Reed, Orr et al. 2013). Commonly used adjuvants include the insoluble aluminum salts adjuvant and the water in oil emulsions, introduced by Freund. Both adjuvants are designed to extend the duration of antigen persistence at the injection site while increasing inflammation to recruit antigen presenting cells (O'Hagan and De Gregorio 2009). A summary of their roles has been provided in Table 1.

Table 2. Roles of adjuvants (modified from (Reed, Orr et al. 2013)

Essential roles of adjuvants
1. Dose sparing
2. Enabling a more rapid immune response
3. Immune response broadening (via cross-reactivity)
4. Developing vaccines for effective T cell responses

Adjuvants have been grouped in classes to provide a clearer description of how they work. These classes include 'delivery systems', and 'immune potentiators'. Delivery systems refer to adjuvants whose main purpose is to deliver antigens to immune cells. Immune potentiators are the alternative group that has direct effects on the immune cells themselves, providing them means of activation (O'Hagan and De Gregorio 2009).

2) Fusion proteins as adjuvants

There is an understanding that many adjuvants activate the host immune system via TLR-mediated signaling through PAMP recognition (Janeway 1989). Therefore, it was surmised that the physical linking of a PAMP to an antigen would increase the immunogenicity of said antigen. A common example of a recombinant fusion protein used as an adjuvant is flagellin. Genetically fusing an

antigen of interest to flagellin increases immunogenicity and the protective capacity of the antigen (Huleatt, Nakaar et al. 2008). *In vitro*, proteins fused with bacterial flagellum were able to mature APCs (antigen presenting cells) and mature APCS were able to produce cytokines capable of inducing inflammation (Cuadros, Lopez-Hernandez et al. 2004). *In vivo*, FlaB was shown to boost mucosal and systemic immunity in mice (Lee, Kim et al. 2006). In light of this discovery, other proteins could also be genetically fused and physically linked to antigens of interest to bolster their immunogenicity.

5. Solubility of recombinant proteins

1) Inclusion bodies

Recombinant proteins do not require post-translational modification and thus, an expression system using a bioreactor such as *E. coli* or yeast are commonly used in the production of such proteins. However, an overall problem in recombinant protein production is the aggregation of proteins into inclusion bodies (Fahnert, Lilie et al. 2004), a major flaw in utilizing *E. coli* as bioreactors. Because inclusion bodies are considered to have little biological activity and the refolding process is time-consuming and requires additional labor, soluble recombinant protein expression must be prioritized. This aggregation of recombinant protein appears to be due to the high expression levels seen in *E. coli* along with the nature of the recombinant protein not originating from the expression host and being considered “non-native” (Lilie, Schwarz et al. 1998).

Thus, recombinant proteins of mammalian origin can be a waste of time and effort to purify in high yield as a soluble form (Galloway, Sowden et al. 2003). The production of inclusion bodies has some positive attributes like high levels of protein expression and protection against degradation (Singh, Panda et al. 2005). However, the main and most important detracting point from inclusion body formation is that inclusion bodies do not have biological activity. In order to reestablish the lost biological activity, inclusion bodies require solubilization, refolding, and purification procedures (Singh, Panda et al. 2005). However, the best-case scenario is to produce a high ratio of soluble to insoluble proteins and avoiding refolding steps altogether.

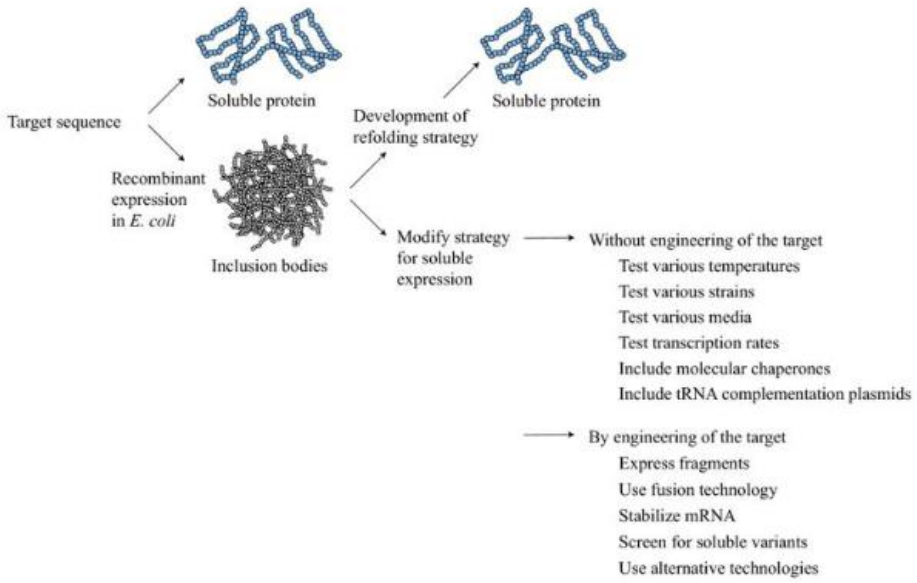

Figure 8. Downstream strategies to obtain soluble recombinant protein (Sørensen and Mortensen 2005)

2) Trigger factor chaperone co-expression

The role of chaperone proteins is to bind to nascent polypeptide chains, prevent inappropriate interactions or aggregations and to help them fold into their native structure. This in turn, reduces inclusion bodies while increasing soluble proteins. There are many kinds of chaperone plasmids which express their respective chaperone protein. Amongst these, pTf16, which expresses trigger factor, was selected in this study to reduce inclusion body production.

Trigger factor (*tig*) is the only ribosome-associated chaperone in bacteria found constitutively expressed in the cytosol and is plentifully found, as it outnumbers ribosomes 5:2 (Crooke, Guthrie et al. 1988). When in action, *tig* transiently associates directly to the ribosome and is available to "catch" the growing polypeptide chains that leave the ribosome itself (Hoffmann, Bukau et al. 2010). The unique shape of *tig* prevents inappropriate interactions along with delaying the folding of the protein. Upon release of *tig* the nascent chains fold spontaneously or must require further folding assistance from other downstream chaperones such as DnaK and its co-chaperone DnaJ or GroEL with its co-chaperone GroES (Hoffmann, Bukau et al. 2010).

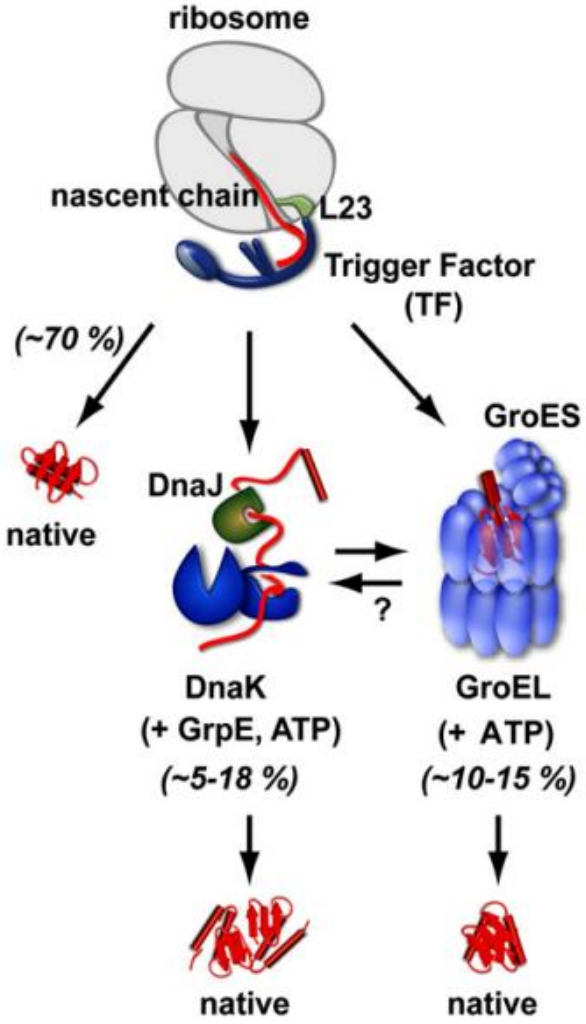

Figure 9. The role of trigger factor (*tig*) chaperone in folding nascent protein polypeptides (Hoffmann, Bukau et al. 2010)

3) Other physiological factors

Besides the use of a chaperone to aid in producing soluble recombinant proteins, there are other physiological factors that play a role in preventing inclusion bodies. These other physiological factors include growth and induction temperatures, growth phase at expression induction, and IPTG induction concentrations.

Aggregates of recombinant proteins were observed in *E. coli* that were grown at higher temperatures, such as at 37 °C, but not in *E. coli* that were grown at 23-30 °C. In *E.coli* the formation of soluble recombinant proteins is favored by lower growth temperatures (Schein 1989). Expression of soluble protein can be enhanced greatly by reducing temperatures of induction as well (Galloway, Sowden et al. 2003).

Besides temperature-based factors, the yield of expressed soluble recombinant proteins can be affected by manipulating the growth phase of induction. Recombinant protein expression protocols call for induction during the mid-log phase with the reasoning that the culture's growth is rapid and thus the protein translation would be at its height (Galloway, Sowden et al. 2003). It appears that formation of aggregated proteins are due to an accumulation of high concentrations of folding intermediates or the chaperones being oversaturated (Sørensen and Mortensen 2005).

IPTG is often used to induce the expression of recombinant proteins with most agreeing that induction with lower concentrations decreases the recovery of soluble protein. Typically, low concentrations of inducers are used in order to avoid oversaturation of the cell's machinery and the chaperone as oversaturation would lead to mis-folded aggregates, otherwise known as inclusion bodies (Kaur, Kumar et al. 2018). In fact, induction with 0.1 mM IPTG was shown to maximize the yield of soluble recombinant protein while induction with 1.0 mM IPTG reduced the total yield (Sørensen and Mortensen 2005).

III. Materials and Methods

1. Preparation of protein

1) Plasmids and strains

S0 was selected as the representative subunit for PEDV due to its cross-reactivity across non-INDEL PEDV strains (Li, Li et al. 2017). As such, the recombinant proteins produced in this study were S0, S0 fused with one mC4d (S0-mC4d1), S0 fused with two tandem repeats of mC4d (S0-mC4d2) and free mC4d. The final recombinant protein plasmid maps can be seen in figure 10. S0-mC4d1, S0-mC4d2, and free mC4d were cloned into the pET28a (+) (Novagen, USA) vector by using the *Nhe* I and *Xho* I restriction enzyme sites, respectively. The pET28a (+) vectors and inserts were digested with *BamHI* and *Xho* I and *Bgl* II and *Xho* I, respectively, overnight at 37 ℃. S0 was inserted into pET28a (+) using the *NheI* and *XhoI* restriction enzyme sites, respectively. To create the fusion proteins S0-mC4d1 and S0-mC4d2, pET28a (+) containing S0 was first opened with *BamHI* and *XhoI*. mC4d inserts contained the restriction enzyme sites for *BglII* and *XhoI*. *BamHI* and *BglII* are isocaudomers and thus may stick together, as seen in figure 10. Within the mC4d insert a second restriction enzyme site for *BamHI* down-stream from *BglII* was included to repeat the process for the mC4d tandem repeat to create S0-mC4d2. The cloning scheme is represented in figure 11.

After digestion, genes were cloned into pET28a (+) vectors using T4 DNA ligase (NEB, USA). The target genes transferred into pET28a (+) vectors were confirmed via size confirmation after gel electrophoresis (2% agarose gel) and visualized with ChemiDoc™, along with Sanger sequencing. No mutations were induced.

The bioreactor selected for this study was the expression host *E. coli* BL21 (DE3). *E. coli* are useful to produce recombinant proteins due to their easy expression system, cheapness, ability to reach high densities of growth very quickly, and the fact that *E. coli* have well-studied genetics with tools that are already available for the use in *E. coli* (Sørensen and Mortensen 2005). In addition, the BL21(DE3) competent cell was selected as it is a T7 expression strain from the lysogens of bacteriophage DE3. As such, they carry the chromosomal copy of T7 RNA polymerase under the control of lacUV5, which expression can be easily induced through IPTG. Expression vectors were transformed into *E. coli* BL21 (DE3) competent cells (Invitrogen, USA) through heat shock transformation at 42°C for 90 seconds. The transformation was confirmed via sequencing and no mutations were induced. Proteins were expressed from recombinant *E. coli* under the control of the *Lac* operon induced by IPTG (Calbiochem, USA). The primers for confirmation of the target gene were the T7 promoter (5'-TAATACGACTCACTATAGGG-3') and the T7 terminator (5'-GCTAGTTATTGCTCAGCGG-3').

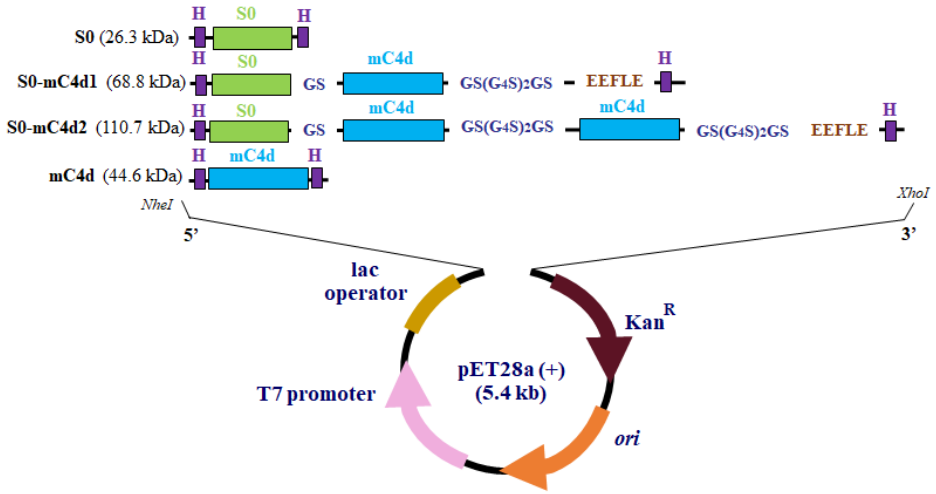

Figure 10. Vector construction scheme containing characteristics of the expression vector, placement of genetic regions of interest, and expected sizes of the target protein sizes.

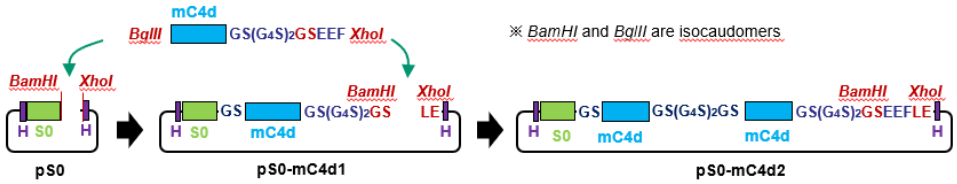

Figure 11. pET28a (+) – S0 – mC4d recombinant protein vector construction scheme

The chaperone plasmid used was pTf16 (TaKaRa, Japan). Plasmids were transformed into the *E. coli* BL21 (DE3)/pTf16 competent cell, which is designed to produce *tig* (trigger factor chaperone), under control of the L-arabinose inducible promoter, *araB*.

2) Recombinant protein expression

A seed culture was prepared by inoculation with a single colony of transformed recombinant *E.coli* and grown overnight in Lysogeny Broth (LB) (BD, USA) containing kanamycin (1000 μg/mL) and chloroamphenicol (2000 μg/mL). 500 mL of LB broth containing 1000 μg/mL of kanamycin was inoculated with 0.1% of the seed culture. For chaperone co-expression, the seed culture was prepared by inoculating a single colony of recombinant *E. coli* and grown overnight in LB broth (BD, USA) containing kanamycin (1000 μg/mL) and chloroamphenicol (2000 μg/mL) followed by adding 1000x L-arabinose for the induction of chaperone proteins. Cells were grown in a shaking incubator at

37 °C and 230 rpm and with growth monitored by spectrophotometer. Once A_{600} of the culture reached the set point, target proteins were induced by adding 0.1 mM IPTG at 15 °C and 150 rpm for 20 hours.

Cells were harvested and washed once with 1x phosphate buffered saline (PBS) before they were lysed with 200x lysozyme on a rotator for 30 minutes at 37 °C. Cells were then disrupted on ice by sonication (VCX 750, SONICS, USA) for 3 minutes of 2 seconds on/5 seconds off, amp 40%. Following centrifugation at 12,000 rpm for 15 minutes, supernatants were collected as a soluble fraction, while pellets were solubilized using 50 mM Tris-Cl, 2 M Urea, pH 12.5 buffer and collected as an insoluble fraction.

3) Ni-NTA affinity chromatography

The clear supernatant from the previous sonication step of the 500 mL culture was purified by using His-tag affinity chromatography. Before purification crude protein was filtered with a 0.45 μm syringe filter (Sigma, USA) to remove cell debris.

The composition of the various buffers used for Ni-NTA affinity chromatography is shown in Table 2. The purification process followed the generalized protocol for Ni-NTA affinity chromatography (Crowe, Masone et al. 1995). Briefly, His-bound resin (Thermo Scientific, USA; 3 mL) was packed into a column for use with the soluble protein. His-bound resin was equilibrated with 2 volumes of binding buffer and charged with 5 volumes of charging buffer.

After washing with 5 volumes to remove uncharged nickel ions, the column was loaded with crude protein. Then, the column was washed with washing buffer containing different imidazole (IMD) concentrations to remove non-specific proteins. The 6x His-tag bearing recombinant protein was eluted with elution buffer. Each fraction was analyzed via SDS-PAGE (sodium dodecyl sulfate-polyacrylamide gel electrophoresis) for purification quality and relative purity of the eluted protein.

Next, eluted protein was dialyzed against 3 L of 1x PBS at 4 °C for 20 hours with 3 fresh PBS changes to remove elution buffer salts. Following dialysis, samples were concentrated using Amicon ultra-15 centrifugal filters (Merck, Germany).

Table 3. Buffer compositions for Ni-NTA affinity chromatography

Buffer		Imidazole	Tris-Cl	NaCl	$NiSO_4$	EDTA	pH	Volume
Charging buffer		-	-	-	50 mM	-	-	5
Binding buffer		5 mM	20 mM	0.5 M	-		7.9	5
Washing buffer	1	5 mM						5
	2	10 mM						5
	3	20 mM						5
Elution buffer		300 mM						5
Strip buffer		-				100 mM		5

* Volume = resin volume

4) SDS-PAGE

Protein expression was analyzed using band intensity and expression purity levels were determined using the percentages of target bands within the total bands of each lane on SDS-PAGE. SDS-PAGE consisted of 5% stacking gels and 12% resolving gels under a reducing condition and run in a Mini-PROTEAN electrophoresis system (BioRad, USA). Gels were stained with Coomassie Blue R250 (AMRESCO, USA). A representative sample of each expression step was collected for SDS-PAGE (Stacking at 80 V for 30 min, Resolving at 120 V for 120 min). Relative band intensity was displayed and quantified by the Image Lab statistical software (Bio-Rad, USA).

5) Quantification of recombinant proteins

Concentrated proteins were quantified by at first producing a standard curve using Bovine Serum Albumin (BSA). After the standard curve was created, 20μL of each recombinant protein was loaded in SDS-PAGE. The band densities of the recombinant proteins were analyzed and plotted based on the concentration and associated band densities of the BSA standard curve.

2. Optimization of protein expression conditions

1) Sample preparation

A seed culture was prepared by inoculation with a single colony of transformed recombinant *E. coli* BL21 (DE3) and grown overnight in LB broth (BD, USA) containing kanamycin (1000 μg/mL) and chloroamphenicol (2000 μg/mL). A total of 8 100 mL Erlenmeyer flasks with 25 mL of LB broth containing kanamycin and chloroamphenicol was inoculated with 0.1 % of the seed culture. For *tig* chaperone optimization, addition of 1000x L-arabinose was applied to half of the flasks. Each recombinant protein was added to two of the flasks, one with L-arabinose and one without L-arabinose induction. Cells were grown in a shaking incubator at 37 °C and 230 rpm and optical densities were monitored by spectrophotometer. Once A_{600} = 0.4 target proteins were induced by adding 0.1 mM IPTG in each flask. Subsequent to IPTG induction, flasks were incubated at 15 °C and 150 rpm for 20 hours. Cells were harvested and

washed once with 1 x PBS before they were lysed with 200x lysosome on a rotator for 30 minutes at 37 °C. Cells were then disrupted on ice by sonication (VCX 750, SONICS, USA) for 1 minute of 2 seconds on/5 seconds off at amp 23%. The inclusion body pellet and soluble supernatant were separated by centrifugation at 12,000 rpm for 15 minutes.

For determining of optimal A_{600} and IPTG induction concentrations, a similar protocol was performed with a total of 6 100 mL Erlenmeyer flasks with 25 mL of LB broth containing kanamycin and chloroamphenicol, inoculated with 0.1% of the seed culture. For chaperone co-expression, 1000x L-arabinose was added for the induction of chaperone proteins. Once A_{600} of the culture reached either 0.4~0.6, for three flasks, or 2.0 for the remaining three flasks, target proteins were induced by adding 0.1 mM, 0.5 mM, and 1.0 mM IPTG in each of the different flasks. At this point, the cell disruption and separation of inclusion bodies with soluble supernatant is as was previously described.

2) Western Blot analysis

Western blot assays were performed by first running proteins in SDS-PAGE and then transferring them to a nitrocellulose membrane (Whatman, USA) in an XCell II™ Blot Module (Invitrogen, USA). After blocking the membrane with Tris buffered saline with Tween 20 (TBST) and 5% skim milk (BD/Difco, USA) overnight at 4°C, the membrane was probed with rabbit anti-His monoclonal antibodies (abcam, UK) in TBST at a dilution factor of 1:2,000 for 1 hour at RT.

The membrane was washed with TBST 3 times and the second antibody, HRP-conjugated goat anti-rabbit IgG (abcam, UK) diluted at a factor of 1:5,000 in TBST and 2.5% skim milk, was rotated with the membrane for 1 hour at room temperature (RT). After washing for 3 times, detection of horseradish peroxidase (HRP) was done through an ECL (enhanced chemiluminescence) detection kit (GE Healthcare, Sweden).

3) Densitometer analysis

Measurements of SDS-PAGE band volumes were conducted using the ImageLab™ Software (Bio-Rad, USA). SDS-PAGE gels were visualized using the ChemiDoc™ XRS$^+$ (Bio-Rad, USA) molecular imager® and the ImageLab™ program that was installed together. Volumes were generated by manually selecting each lane and the band of interest before analyzing the band.

3. *In vivo* immunization

1) Mouse immunization

To evaluate the adjuvanticity of mouse C4d, mice were immunized with S0, S0-mC4d1, S0-mC4d2, and two different S0 and mC4d mixture groups with CFA (complete Freund's adjuvant) and IFA (incomplete Freund's adjuvant) via the intramuscular route for 6 weeks. The immunization schedule consisted of a primary injection using CFA and two booster injections each 2 weeks apart (at 2 weeks and 4 weeks post primary injection) with IFA. Both the humoral immune

response, seen through indirect IgG ELISA, and the cellular immune response, seen through splenocytes on ELISpot assay, were studied to determine relative immunogenicity of target proteins. Indirect ELISA for S0-specific IgG end point antibody titers was conducted using antisera at 7 days, 2 weeks, 4 weeks, and 6 weeks. In addition, T cells from the spleen were removed from mice after 6 weeks post injection and analyzed.

Mice were purchased from KoaTech (Korea) and the experiment was performed in accordance with the guidelines for the care and use of laboratory animals under the approval of the animal ethics committee at Seoul National University (SNU-161114-8).

4 female BALB/c mice that were 6 weeks old were provided with free access to food and water under standard pathogen-free conditions. The detailed immunization schedule can be seen in figure 12. After 1 week of acclimatization, mice were immunized intramuscularly through the right gastrocnemius muscle with recombinant protein suspended in 1x PBS three times at two-week intervals. CFA and IFA were mixed with antigens for the priming and boosting of mice respectively. General information of the mouse immunization such as organization of groups and dosages are provided in Table 3.

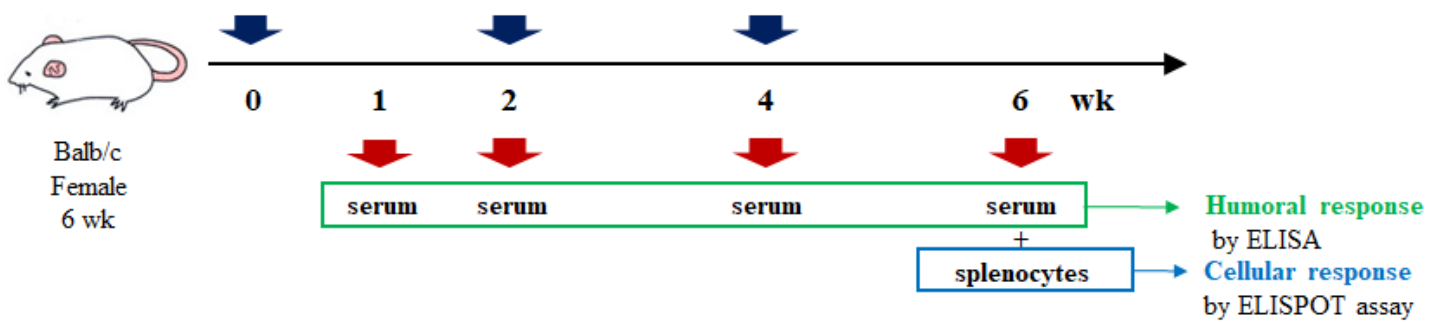

Figure 12. *In vivo* immunization schedule and overall design.

Table 4. Immunization scheme

No.	Group	Mice	Dose		Note
			nmol/mouse	µg/mouse	
1	Untreated	4	---	---	Negative control
2	S0	4	0.12	3.0	S0 antigen alone
3	S0-mC4d1	4		8.0	S0 fused with one mC4d
4	S0-mC4d2	4		12.9	S0 fused with two mC4d tandem repeats
5	S0 + mC4d	4	0.12 + 0.12	3.0 + 5.2	S0 mixed with mC4d
6	S0 + mC4d (x2)	4	0.12 + 0.24	3.0 + 10.4	S0 mixed with mC4d two times

2) Blood extraction

Blood samples of immunized were collected at 1, 2, 4, and 6 weeks after immunization. Each blood sample was collected before immunization when applicable. Blood sampling was conducted by piercing the cheek with a syringe and allowing blood to drip into microtainers (BD, USA) followed by isolation of serum from blood via centrifugation at 14,000 rpm for 3 minutes, serum was stored at 4 °C until later use.

3) S0-specific indirect ELISA

The induction of antigen specific serum IgG level was measured by indirect ELISA. 96 well immunoplates (SPL life science, Korea) were coated with 10 μg/mL of purified recombinant S0 in 0.05 M carbonate-bicarbonate buffer (pH 9.6) (Sigma, USA) (100 μg/well) at 37 °C for 2 hours. After 1 wash with PBS (200 μg/well), plates were blocked with 0.5% skim milk in 1x PBST (100 μL/well) at room temperature for 1 hour. After washing with PBST (200 μL/well) once, serum originally diluted at 1:50 was serially diluted down the plate rows and incubated at 37 °C for 2 hours. After 3 washes with PBST (200 μL/well), HRP conjugated goat anti-mouse IgG 1:4000 was used as the secondary antibody (100 μL/well). After incubation at room temperature for 1 hour, the 96 well immunoplates were washed with PBST 3 times (200 μL/well). Then, plates were incubated with a TMB substrate solution (Sigma, USA) (100 μL/well) at room temperature for 30 minutes without light interference and the

reaction was stopped by added stop solution (1 M H_2SO_4; 100 μL/well). Absorbance at 450 nm was measured in an Infinite 200 PRO microplate reader (TECAN, Switzerland). ELISA results were expressed as the endpoint titer.

4) Spleen isolation and detection of auto-reactive helper T-cells

Spleens were isolated from 2 mice per group at 6 weeks after immunization. The spleen was stored in 5 mL of pre-warmed RPMI 1640 medium (Gibco, USA) containing 10% FBS (GenDEPOT, USA) and 5% P/S until use. The spleen was placed on an empty petri dish and ground using the plunger end of a syringe. Cells were then filtered through a cell strainer (Falcon, USA) with an extra 5 mL medium. After centrifugation at 1,000 rpm for 5 minutes, supernatant was removed by suction and 1 mL ACK lysis buffer (Gibco, USA) was added. After incubation on ice for 10 minutes, 5 mL of medium was added followed by centrifugation at 1,000 rpm for 5 minutes. After the supernatant was removed, cells were resuspended in cRPMI.

5) ELISpot analysis

IL-4 + ELISpot plate purchased from RnD SYSTEMS® kit from R&D Systems, USA. S0, mouse C4d, and mouse C3d was diluted in cRPMI 1640. With 100μL added to each well, each well contained 5 μg as a final concentration after 100μL cell suspensions at a final density of 1 x 10^6 was added. Plates were then incubated at 37 °C in a 5% CO_2 humidified incubator for 72 hours (3 days). For the detection of antibody, cell suspensions prepared as

instructed by the kits. Briefly, the wells were aspirated then each well was washed twice with dH_20 and then washed three times with wash buffer provided with the kit. After the prepared Detection Antibody Solution was added, the lid was replaced and incubated for 2 hours at RT. After washed again with wash buffer, the HRP was added and then incubated once more. After incubation and more washes, the substrate solution was added, and spotting was monitored.

ELISpot wells were punched onto Eli.Foil (A.EL.VIS, USA) using Eli.Punch tool (A.EL.VIS, USA) and spots on each well were photographed using the A.EL.VIS ELISPOT software called Eli Analyze (A.EL.VIS, USA). Using the images from Eli Analyze, exact spot measurements were counted using the naked eye.

4. Statistical analysis

All results are expressed as mean $\pm$ standard deviation (SD). Statistical significance was assessed using paired samples Student's T-test and Bonferroni post hoc test. All statistical analysis was performed using GraphPad PRISM software (GraphPad Software, Inc.). All statistical significance is denoted by *P < 0.05, **P < 0.01, and ***P < 0.001.

IV . Results and Discussion

1. Production of soluble recombinant fusion protein in *E. coli*

1) Vector construction

From the T-cell epitope database analysis, C4d had become a candidate as a T-cell epitope donor. Thus, a recombinant plasmid was designed using C4d as the adjuvant which would be fused to the S0 spike protein of PEDV.

Briefly, all genetic inserts of the recombinant proteins were inserted within the *NheI* and *XhoI* restriction enzyme sites of the pET28a (+) plasmid, a suitable T7 expression plasmid. C4d tandem repeats were added behind the S0 sequence by taking advantage of the same sticky ends of *BamHI* and *BglII*. Each recombinant gene has a 6x his tag on both ends and each mC4d insert contains a GS (glycine serine) linker. For a more detailed description of the cloning process, refer to the corresponding methods and materials section.

The cloning process was confirmed through two methods, restriction enzyme digestion and through sequencing. After digestion with *NheI* and *XhoI*, the digested plasmids were run through a 1% agarose gel with electrophoresis, as seen in figure 13. The cut pET28a (+) vector's expected size is 5.4 kb and each

of the inserts' sizes are 0.6 kb for S0, 1.2 kb for mC4d, 1.8 kb for S0-mC4d1, and 3.0 kb for S0-mC4d2.

Visualization of the bands show that each of the recombinant plasmids were cut to the correct size indicating that the cloning proceeded as planned and was a success as shown in figure 13. Sequencing was performed through Sanger sequencing at the NICEM facility at Seoul National University. The sequencing primers were the universal primers T7 and SP6, respectively. Sequenced obtained through Sanger sequencing were compared with template sequences and analyzed through BLAST (Basic Local Alignment Search Tool, NCBI, USA) (data not shown). Sanger sequencing revealed that the identity of the samples matched the template sequences for S0-mC4d1, S0-mC4d2, and mC4d alone at a match rate of 100%.

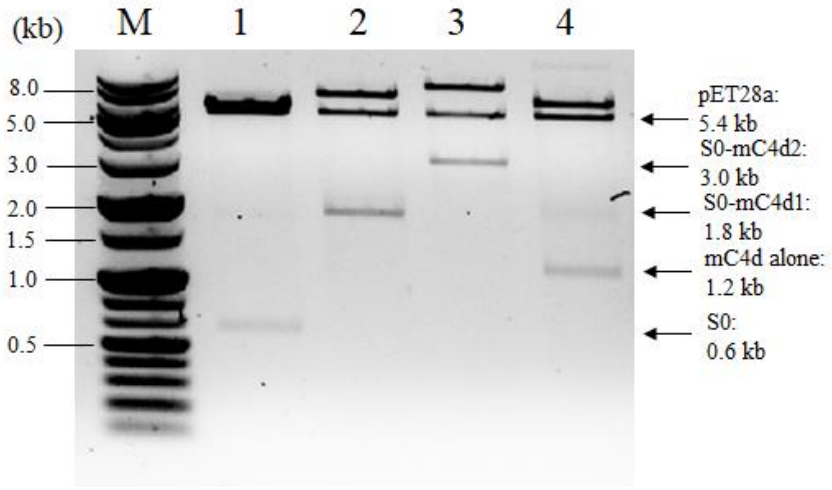

Figure 13. Confirmation of cloning of mouse C4d into pET28a (+)–S0 in a series through restriction enzyme digestion (*NheI* and *XhoI*) run in 1% agarose gel. (A) S0 is separated from pET28a (+) with digestion with *NheI* and *XhoI*, (B) restriction enzyme digestion (*NheI* and *XhoI*) of the recombinant plasmid pET28a (+)–S0–mC4d1, (C) restriction enzyme digestion (*NheI* and *XhoI*) of the recombinant plasmid pET28a (+)–S0–mC4d2, and (D) restriction enzyme digestion (*NheI* and *XhoI*) of the recombinant plasmid pET28a (+)-mC4d alone (A) Lanes: M, 1kb DNA ladder; 1, pET28a (+)-S0 (B) Lanes: M, 1kb DNA ladder, 1, pET28a (+)–S0–mC4d1; (C) Lanes: M, 1kb DNA ladder; 1, pET28a (+)–S0–mC4d2; (D) Lanes: M, 1kb DNA ladder; 1, pET28a (+) -mC4d alone Band size of mC4d alone, 1.2 kb; pET28a (+), 5.3 kb, S0-mC4d1, 1.8 kb, S0-mC4d2, 3.0 kb.

Gel image reveals the presence of "ghost bands". Upon further inspection of the electrophoresis gels, the un-cut plasmids had a pronounced band volume. Rather than simply being un-cut plasmids, as they were given sufficient time for digestion, these bands could very well be "ghost bands". Ghost bands may often be caused by supercoiled DNA during the plasmid preparation. As they are in supercoiled form, the restriction enzymes sites are obscured, and they are not cut

by the restriction enzymes. The existence of the ghost bands does not impact the overall study as the point was to see the correct sizes for the inserts and vectors. In the end, three correctly sized bands were visualized and confirmed.

Following the cloning of the recombinant plasmids, each recombinant plasmid was transformed to an expression host, the competent cell *E. coli* BL21 (DE3) (TaKaRa, Japan) through heat-shock transformation.

2) Production of soluble recombinant proteins

After the expression vectors were cloned to the competent cells, the generic protocol for protein expression was followed. Briefly, cells were cultivated until they reached the mid-log phase of growth (A_{600} = 0.4-0.6) and then 0.1 mM IPTG was added to the culture to induce protein expression. After incubation at 15° for 24 hours, cells were disrupted, and the disruption products were separated for SDS-PAGE analysis. As shown in figure 14A, following this procedure caused all recombinant proteins to be expressed within the inclusion body. Densitometer analysis revealed that S0 was expressed completely in the inclusion body, about 99% insoluble. On the other hand, mC4d by itself was able to be expressed 85% in a soluble form. In addition, adding sequentially increasing tandem repeats of S0-mC4d1 and S0-mC4d2 increases the relative solubility of S0, 41% and 62%, respectively. In conclusion, expression of proteins using a generic, plain expression condition produces insoluble S0. The

joining of mC4d to S0 increases the solubility however, even with mC4d conjugation, recombinant proteins remain somewhat insoluble.

The overall goal of recombinant protein expression is to express the proteins as soluble as possible. With this goal in mind, there were three factors that were considered for soluble protein expression. The first factor was the use of a chaperone.

In order to test for the utility of *tig* chaperone, two protein expression conditions were analyzed using SDS-PAGE gels in figure 14A and 14B. Band volumes were quantified, and relative solubility was determined. As shown in figure 14C and 14D, there is a markedly apparent difference in solubility of expressed proteins when the *tig* chaperone is used, versus when the chaperone is not co-expressed with target proteins. S0-mC4d1's solubility increases from 41% to 75% with chaperone assistance. S0-mC4d2 solubility also benefits from chaperone co-expression as evident from its relative solubility increasing from 62% to 98%. Even S0, which is incredibly insoluble, saw an increase of 1% to 60% solubility with chaperone assistance. mC4d was very soluble without chaperone assistance and with chaperone co-expression the solubility of mC4d experienced a slight decrease from 85% to 78%, however the solubility remained relatively high, despite the drop. A compiled table containing all of the percentages of solubility may be referenced in table 5. From this data, it was determined that when *tig* is co-expressed with the recombinant proteins, the solubility of each of the proteins drastically increases regardless of which

recombinant protein is being expressed and thus, the use of a chaperone is imperative to producing soluble recombinant proteins when using the *E. coli* Bl21(DE3) expression host.

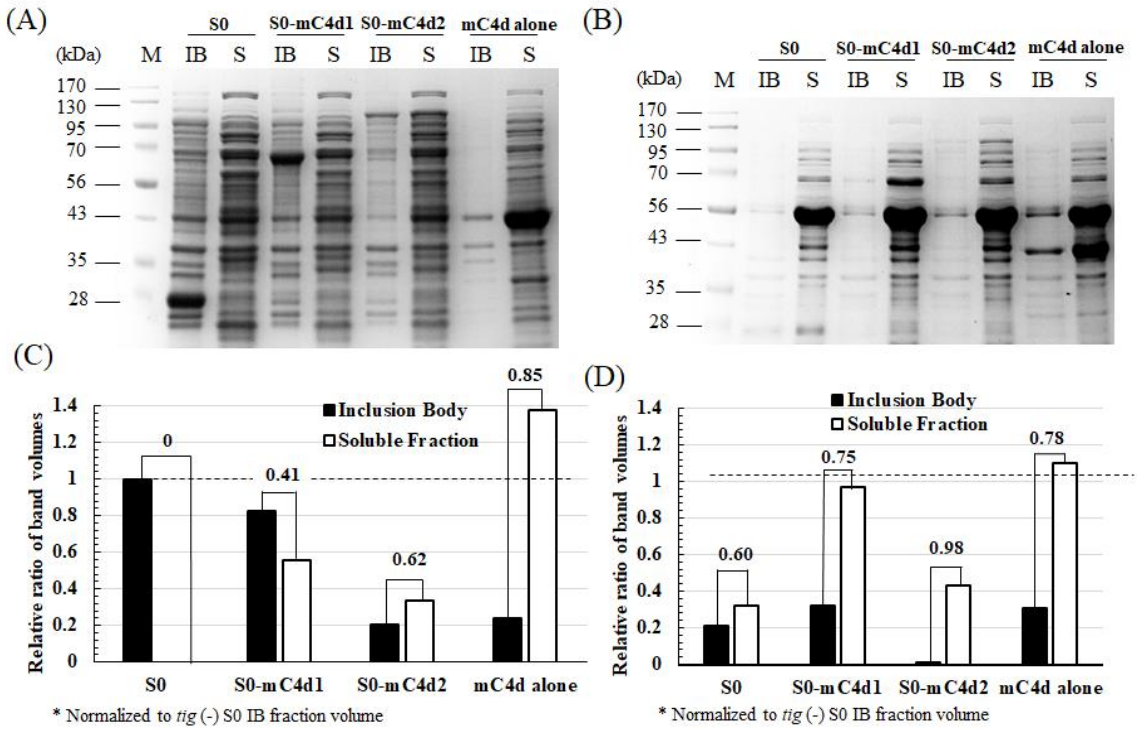

Figure 14. Trigger factor (*tig*) chaperone's effect on solubility of recombinant proteins S0, S0-mC4d1, S0-mC4d2, and mC4d alone with *tig*. Insoluble and soluble fractions of the recombinant proteins (A) without *tig* chaperone and (B) with *tig* chaperone. IB: inclusion body; S: soluble fraction. Molecular weight of S0, 26.3 kDa; S0-mC4d1, 68.8 kDa; S0-mC4d2, 110.7 kDa; mC4d alone, 44.6 kDa

Table 5. Trigger factor chaperone's effect on recombinant protein solubility as a percent.

Target protein	Chaperone condition	% Soluble
S0	*tig* -	0
	tig +	60.0
S0-mC4d1	*tig* -	40.5
	tig +	75
S0-mC4d2	*tig* -	62.0
	tig +	98.2
mC4d	*tig* -	85.3
	tig +	78.1

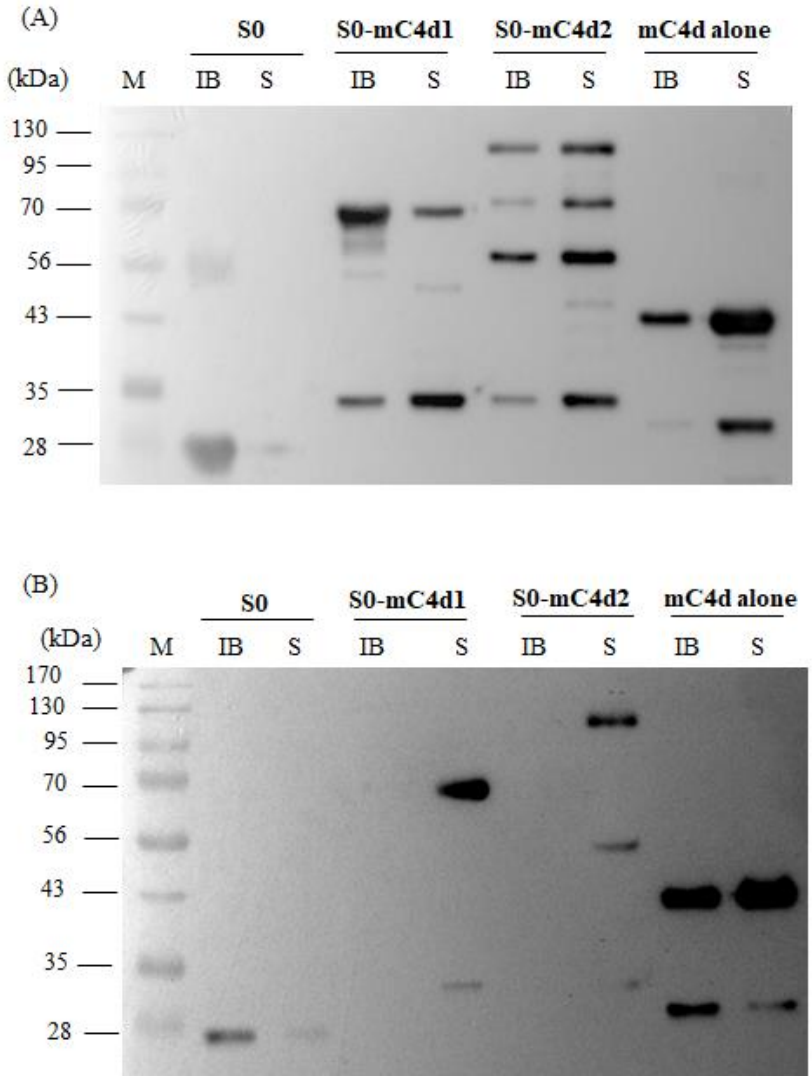

Figure 15. Western blot analysis of soluble recombinant protein expression in *E. coli* (A) with or (B) without co-expression with *tig* chaperone. Lanes: IB, Inclusion body; S, Soluble fraction. Molecular weight of S0, 26.3 kDa; S0-mC4d1, 68.8 kDa, S0-mC4d2, 110.7 kDa; mC4d, 44.6 kDa.

A western blot using the *tig* chaperone and *tig* chaperone null samples was done to confirm the identity of each of the IB and soluble fraction bands and determine if they are indeed that of the recombinant proteins. As evidenced by figure 15A and 15B, antibodies were able to detect the 6x His-tags of the recombinant proteins in both gels. By comparing the relative band sizes to the expected protein sizes, each recombinant protein was positively identified. S0, with an expected band size of 26.3 kDa had a band appear on both the – *tig* western blot and in the + *tig* western blot right below the ladder marker of 28 kDa. S0-mC4d1, which is 68.8 kDa in size, had a prominent band appear between 56 kDa and 70 kDa on both blots. In figure 15A, there is a thicker band in the inclusion body lane than in the soluble lane and there are also two bands while in 15B, S0-mC4d1 has two bands in the soluble fraction with the prominent one being the appropriate size. The second band appears to be a residue of degradation in the protein. S0-mC4d2 was expected to be 110.7 kDa in size and the target band appeared between 95 kDa and 130 kDa in 15B. In 15A, the target also appears alongside numerous other bands, once again, showing signs of degradation in the protein sample. Regardless, while viewing figure 15A, S0-mC4d2 has a target band in both the inclusion body and soluble sample lanes but the soluble lane appears to be thicker. In 15B, the only band for S0-mC4d2 appeared in the soluble fraction. mC4d, which has a predicted protein size of 44.6 kDa had a target band which appeared between 35 kDa and 43 kDa. For 15A, which shows expression without *tig*, mC4d had a thicker band in the

soluble fraction showing its ability to be solubility without chaperone assistance. However, when chaperone assistance is provided, mC4d still retains its soluble nature. As such, the western blot provides evidence that the SDS-PAGE gels could be trusted as showing the correct recombinant proteins.

Figure 15A is marked with the presence of multiple bands that are smaller in size than the expected indicating that during protein expression, the proteins appeared to be pre-maturely stopped during the protein making process. However, in 15B, proteins did not have such bands. In conclusion, the chaperone ameliorated the issue of having smaller, chopped up fragments and it was determined that the chaperone will be used in further experiments.

Use of the chaperone greatly enhanced the solubility of the recombinant proteins, however, other aspects of the expression protocol could be optimized to further increase solubility of the target proteins. These other aspects refer to the physiological conditions of growth phase of induction of expression and the amount of IPTG used for induction.

For S0-mC4d1, six samples of differing A_{600} values, and IPTG concentrations were examined for their respective inclusion body and soluble protein ratios (figure 16) on SDS-PAGE gels. Figure 16A and 16B show that when the set point optical density value is $A_{600} = 0.6$, the proteins produced are soluble. On the other hand, in figure 16C and 16D, when the set point optical density value is $A_{600} = 2.0$ the expressed proteins remain in the inclusion body lane.

Manipulating or increasing the IPTG amount used for induction does not appear to greatly affect the solubility of recombinant proteins.

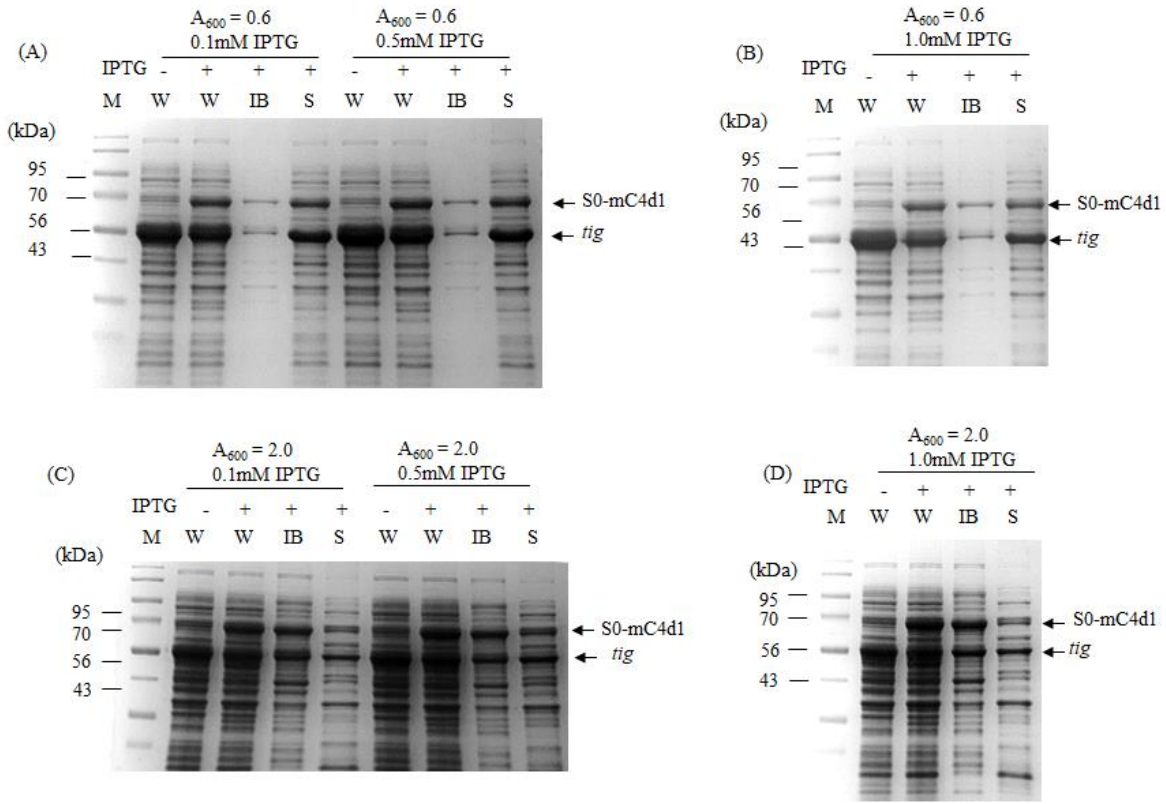

Figure 16. Determination of optimized expression conditions of recombinant S0-mC4d1. S0-mC4d1 was expressed in *E. coli* Bl21 (DE3). Normalized amounts of each sample were analyzed using SDS-PAGE followed by Coomassie Blue staining. M, Marker; W, whole cell lysate; IB, inclusion body; S, soluble fraction. Molecular weight of S0-mC4d1, 68.8 kDa.

In addition, ImageLab© was used to calculate the density of the bands representing the inclusion body and soluble fraction of each sample. Band densities were normalized to be a ratio of the band density of S0-mC4d1's soluble fraction when induced at A_{600} = 0.6 with 0.1 mM IPTG. As seen in figure 17, densitometer analysis supports the visualized gel images where solubility is greatly enhanced when proteins are induced during the mid-log phase of growth rather during the late-log phase or stationary phase. Values from the densitometer analysis were also used to calculate apparent solubility of each condition expression for S0-mC4d1. When protein expression was induced during A_{600} = 0.6, proteins are expressed in a soluble fashion. When given 0.1 mM IPTG, the percentage of solubility is 88%, when using 0.5 mM IPTG it is 87%, and when using 1.0 mM IPTG the solubility is 78% soluble. Between the concentrations of IPTG used, the solubility does not fluctuate. What does cause solubility to be negatively impacted is when protein expression is induced when A_{600} = 2.0. At 0.1 mM IPTG, the protein is only 11% soluble. At 0.5 mM IPTG or 1.0 mM IPTG, the proteins are 17% and 28% soluble, respectively. More than the concentration of the inducer, the most important factor determining solubility is the growth phase at induction. Exact percentages of solubility are shown in the table 6.

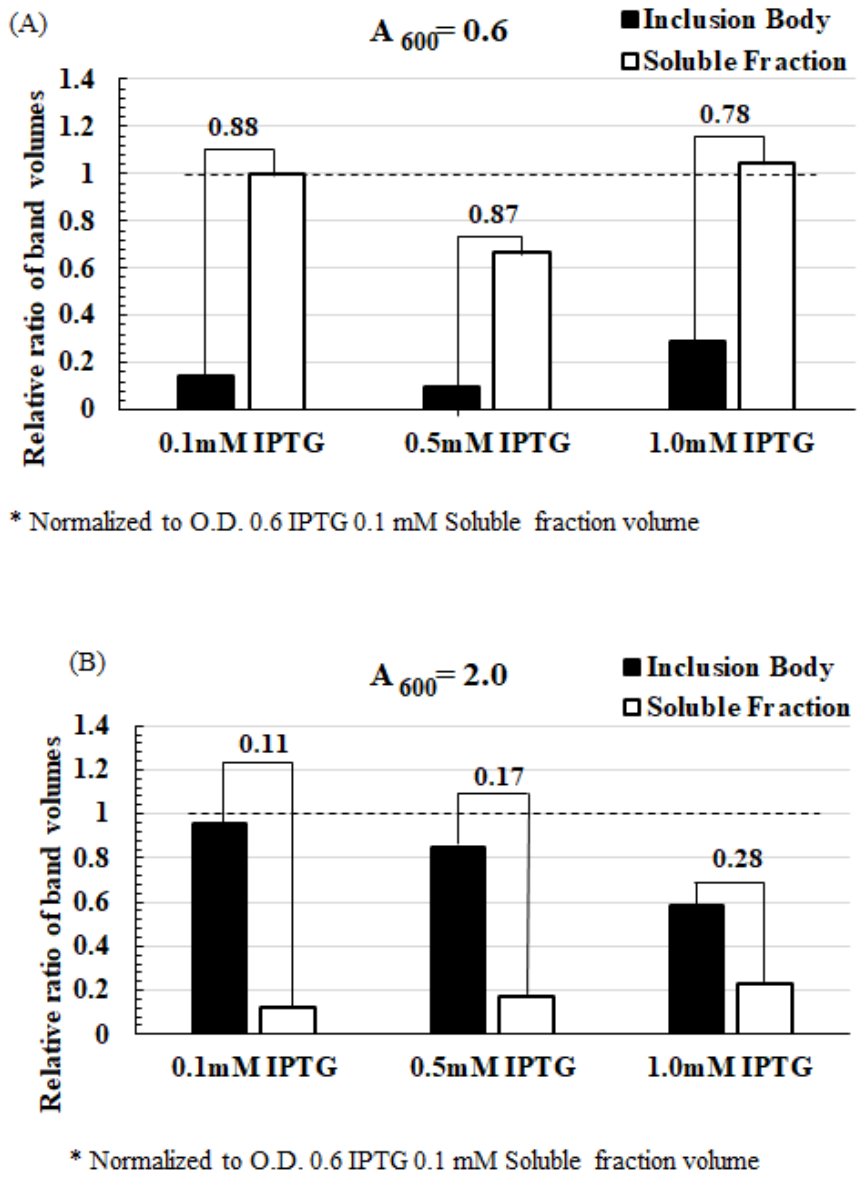

Figure 17. Solubility ratios of S0-mC4d1 through densitometer analysis of S0-mC4d1 from (A) set point optical density at A_{600} = 0.6 and (B) set point optical density at A_{600} = 2.0. Values were normalized to the volume of the soluble fraction at A_{600} = 0.6 with 0.1 mM IPTG.

Table 6. Effects of changes to expression condition variables for S0-mC4d1.

S0-mC4d1	IPTG concentration (mM)	Solubility %
A_{600} = 0.6	0.1	87.7
	0.5	87.0
	1.0	78.5
A_{600} = 2.0	0.1	11.4
	0.5	16.9
	1.0	28.3

The fusion protein S0-mC4d2 was the next protein to be optimized for soluble expression and the protocol for expression was identical to that of S0-mC4d1. Figure 18A and 18B show that when the set point optical density value is A_{600} = 0.6, the proteins produced are soluble but when the A_{600} is 2.0, the target proteins are found along with the inclusion bodies as shown in figure 18C and 18D. This result was expected as a precedent had been made while optimizing the protein expression of S0-mC4d1.

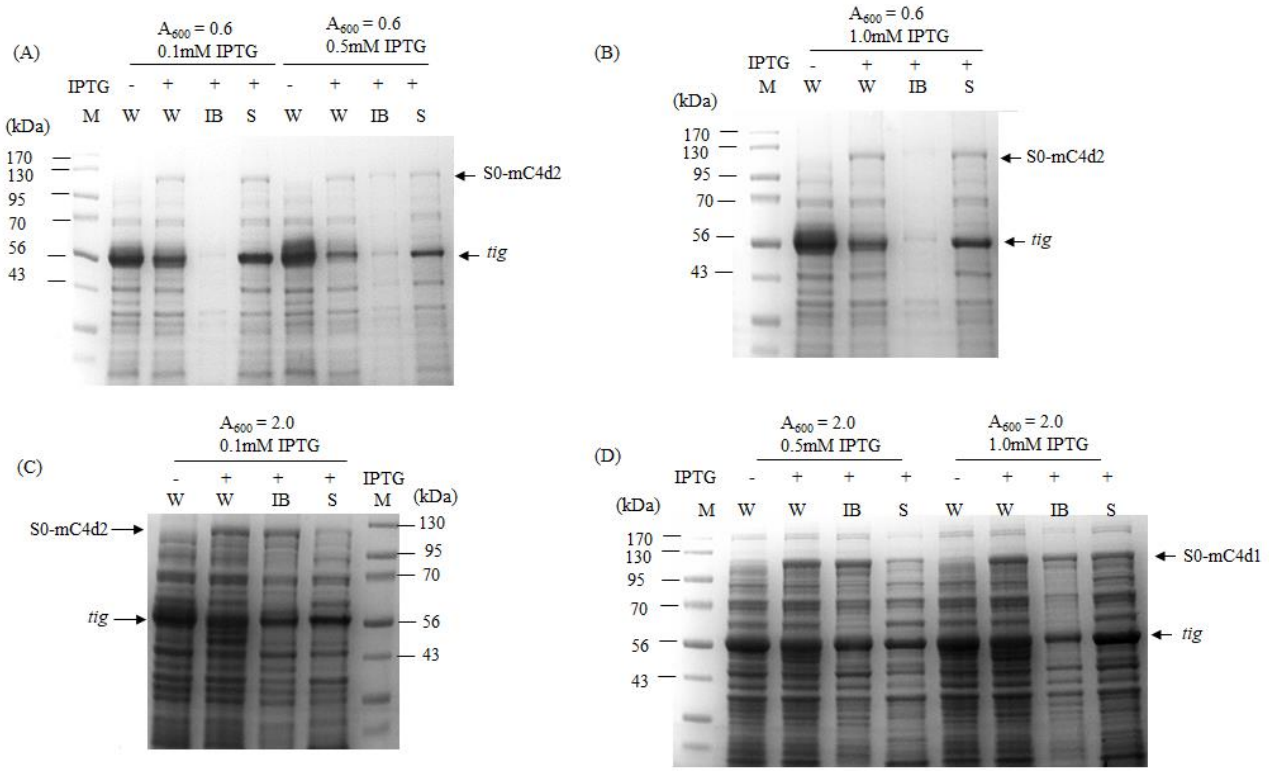

Figure 18. Determination of optimized expression conditions of recombinant S0-mC4d2. S0-mC4d2 was expressed in *E. coli* Bl21 (DE3). Normalized amounts of each sample were analyzed using SDS-PAGE followed by Coomassie blue staining. M, Marker; W, whole cell lysate; IB, inclusion body; S, soluble fraction. Molecular weight of S0-mC4d2, 110.7 kDa.

After visualization of the gels were completed, the densities of the bands were determined and graphed in figure 19. As expected, the A_{600} = 0.6 graph, which represents induction of target proteins during the mid-log phase, shows mainly soluble proteins such as when using 0.1 mM IPTG, the proteins are 99% soluble, when using 0.5 mM IPTG, the proteins are 71% soluble, and when using 1.0 mM IPTG the proteins are once again 99% soluble as well. When proteins are induced in the late-log phase/stationary phase, the inclusion body bars dominate, indicating the proteins are insoluble. When using 0.1 mM IPTG to induce proteins during the late-log/stationary phase the percentage of soluble protein was only 19%. Even when the concentration of IPTG was increased to 0.5 mM IPTG or 1.0 mM IPTG, the percentage of soluble proteins is only 43% and 49%, respectively. Table 7 shows the differences in solubility represented as percentage of soluble protein to the total protein expressed in both the inclusion body lane and soluble fraction of each respective sample's lane.

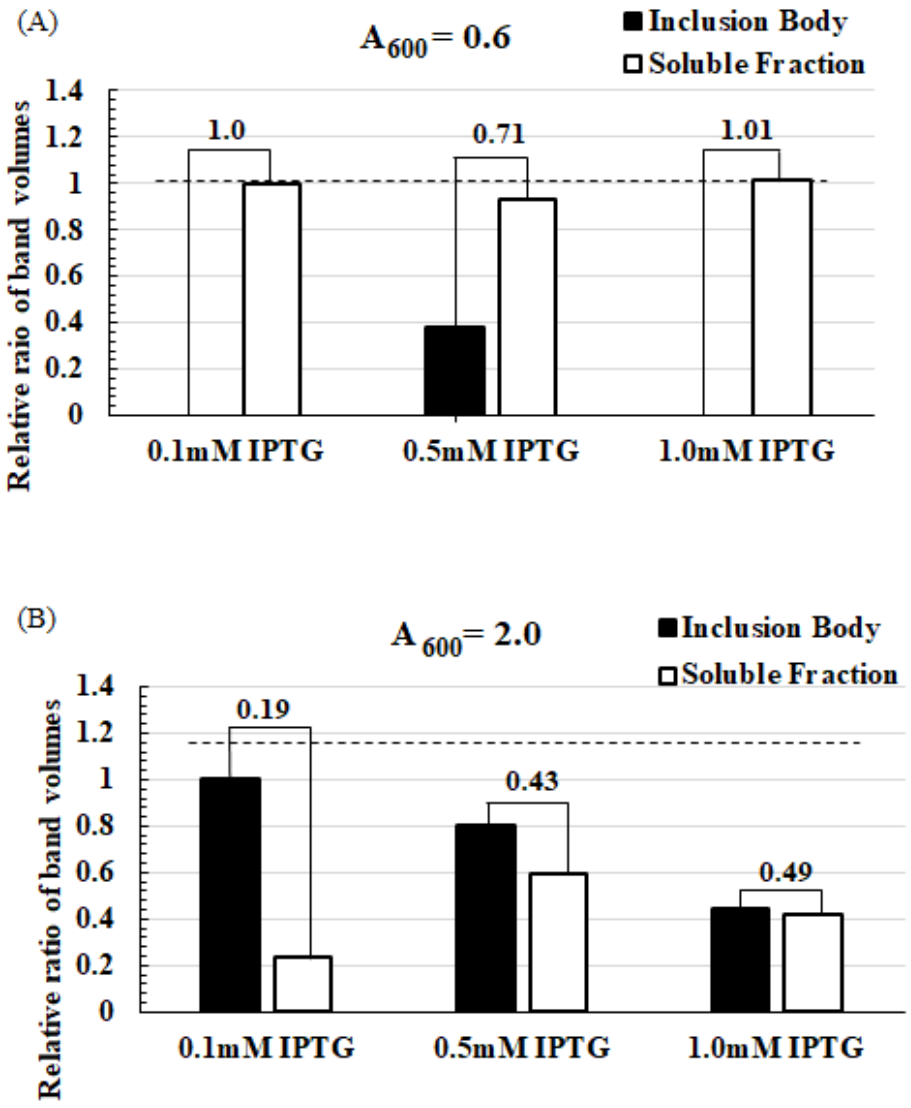

Figure 19. Solubility ratios S0-mC4d2 through densitometer analysis from (A) set point optical density at A_{600} = 0.6 and (B) set point optical density at A_{600} = 2.0. Values were normalized to the volume of the soluble fraction at A_{600} = 0.6 with 0.1 mM IPTG.

Table 7. Effects of changes to expression condition variables for S0-mC4d2.

S0-mC4d2	IPTG concentration (mM)	Solubility %
A_{600} = 0.6	0.1	100
	0.5	71.1
	1.0	100
A_{600} = 2.0	0.1	19.0
	0.5	42.8
	1.0	48.7

Comparison of protein expression for both S0-mC4d1 and S0-mC4d2 during the optimization experiment showed band sizes for S0-mC4d2 were markedly thinner and less obtrusive than S0-mC4d1's bands. This could be due to the fact that recombinant proteins which can be supported by *E. coli* based on sizes as proteins that are larger than 100 kDa have poor expression performance (Kaur, Kumar et al. 2018). It could be assumed that the expression host lost its effectiveness of producing S0-mC4d2, which has a size of 110.7 kDa.

As seen in the results, the most significant factor of soluble protein expression was the phase of growth of bacterial culture at time of induction. Induction during the mid-log phase (A_{600} = 0.4-0.6) means that when proteins are induced,

the metabolic activity is fully increased, meaning recombinant gene expression is on the rise and proteins are being produced. At higher cell densities, the activity of the cells declines as nutrients and resources are used up decreasing gene expression and protein production (Kaur, Kumar et al. 2018). It is favorable to induce proteins earlier to decrease expression of other proteins and make protein purification more efficient. In regard to the optimal concentration of the inducer, for both S0-mC4d1 and S0-mC4d2, the amount of IPTG used to induce protein expression did not greatly affect soluble expression.

In conclusion, the protocol for optimized soluble expression of recombinant protein S0-mC4d1 and S0-mC4d2 utilizes the *tig* chaperone while inducing of protein expression with 0.1 mM IPTG at the mid-log phase (A_{600} = 0.4- 0.6).

3) Expression, purification, and quantification of soluble recombinant proteins

Large scale production of the recombinant protein was accomplished by following the procedure established through the optimization experiments in a 500 mL culture. The large batch of proteins harvested from *E. coli* would then be purified with the intent to immunize mice with said proteins. The protocol to produce recombinant proteins and their subsequent purification process are described in detail in the materials and method section.

The first recombinant protein produced on a large scale was S0-mC4d1. As seen in figure 20, the second whole lysate lane indicates that induction of the

target protein with IPTG was successful, creating the target band at the correct size of 68.8 kDa. This was evident as the target band was located between the marker lanes for 56 kDa and 70 kDa. Samples from the purification process can also be viewed in figure 20. As seen in the sample flow through lane, a small portion of the target protein was eluted out but the proteins that adhered to the column remained bound to the nickel until the elution buffer was added, completely eluting the protein. Most of the contaminants were eluted with the sample flow through and any remaining non-specific bands were washed out in the first wash.

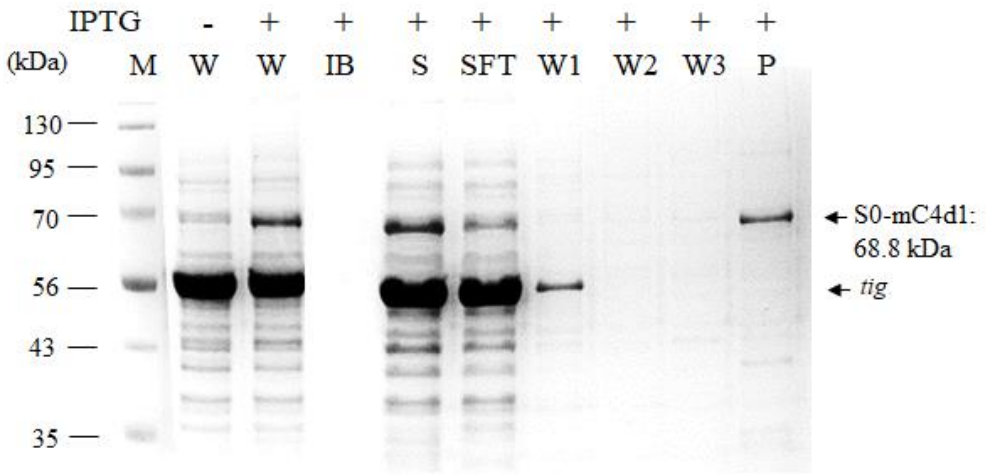

Figure 20. Relative expression and purification of recombinant S0-mC4d1 by Ni-NTA column. Lanes: M, marker; W, whole lysate; IB, inclusion body; S, soluble fraction; SFT, sample flow through; W1, washed fraction 1; W2, washed fraction 2; W3, washed fraction 3; P, purified fraction. Molecular weight of S0-mC4d1, 68.8 kDa.

Next, S0-mC4d2 was produced following an identical protocol with how S0-mC4d1 was produced, as seen in figure 21. As such, a similar result could be seen on the SDS-PAGE gel. After IPTG induction, the target protein band appears, as seen by comparing the two whole lysate lanes. In addition, after sonication, the target proteins were, unsurprisingly, are in the soluble fraction. Of note, during purification a portion of the target proteins were lost in the sample flow through but the proteins that did truly adhere to the column remained there until eluted. This indicates that the purification of S0-mC4d2 was successful. In addition, many of the non-specific bands were eluted out during the first wash with 20 mM IMD (imidazole) producing relatively pure protein samples in the elution buffer.

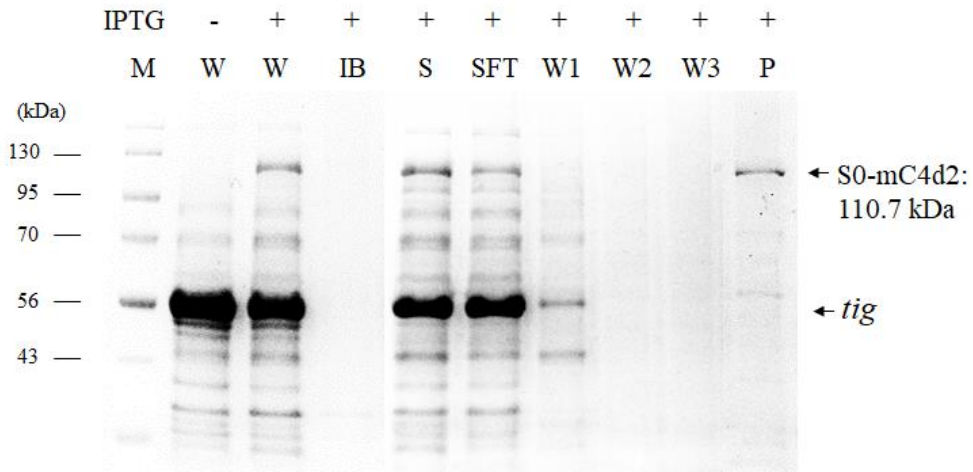

Figure 21. Relative expression and purification of recombinant S0-mC4d2 by Ni-NTA column. Lanes: M, marker; W, whole cell lysate; IB, inclusion body; S, soluble fraction; SFT, sample flow through; W1, washed fraction 1; W2, washed fraction 2; W3, washed fraction 3; P, purified fraction. Molecular weight of S0-mC42, 110.7 kDa.

S0-mC4d2 has as smaller final yield than S0-mC4d1, evidenced in the purified lane of figure 21. This may be caused by the size of the proteins, as the expression host may have more difficulties producing a large protein, which has been previously mentioned. In addition, the loss of protein through the sample flow through decreased the total yield even more resulting in less protein than S0-mC4d1.

Finally, free mC4d was produced as well. Free mC4d was produced with the intent to produce "mixture" control groups in the *in vivo* immunization of mice. The large-scale expression and purification procedure are represented by the SDS-PAGE gel shown in figure 22, which shows each step of the process. The free mC4d would be mixed together with free S0 in order to test the immunogenicity between fusing the recombinant proteins together or mixing them together in a cocktail-like solution. Of note, free mC4d can be produced without many of the hardships of producing the larger, fusion proteins. As seen in figure 22, the amount of mC4d induced by using IPTG is nearly comparable with the amount of chaperone protein produced. During purification the majority of the expression protein adhered to the resin preventing significant yield loss. In addition, after purification, the band size of free mC4d is incredibly thick and bold, indicating a massive yield.

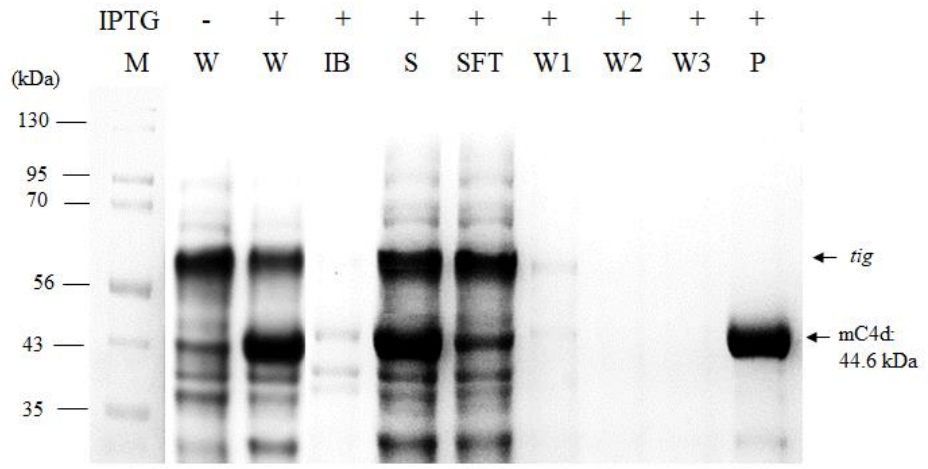

Figure 22. Relative expression and purification of recombinant mC4d by Ni-NTA column. Lanes: M, marker; W, whole cell lysate; IB, inclusion body; S, soluble fraction; SFT, sample flow through; W1, washed fraction 1; W2, washed fraction 2; W3, washed fraction 3; P, purified fraction. Molecular weight of mC4d, 44.6 kDa.

After proteins were purified, the eluted samples were concentrated by centrifugation through filters. As seen in figure 23, concentrated samples were run through an SDS-PAGE and the concentrations of each target protein was determined by comparing the band volumes with known protein concentrations of BSA (bovine serum albumin) derived from a standard curve. The band densities are highly concentrated and are of high purity. The concentrations of each target protein were determined as S0: 0.26 mg/mL, S0-mC4d1: 0.75 mg/mL, S0-mC4d2: 0.52 mg/mL, and free mC4d: 10 mg/mL.

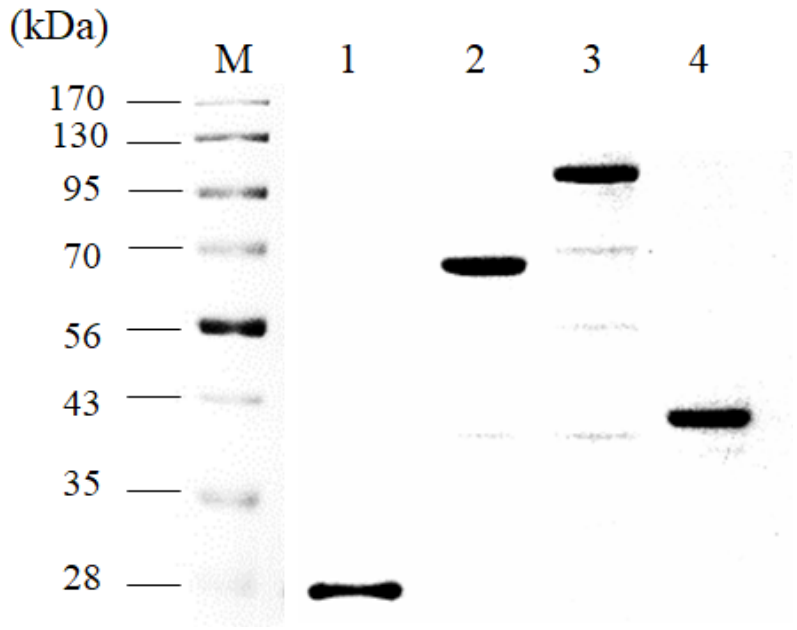

Figure 23. Quantification of pure recombinant proteins. Lanes: M; 1, S0; 2, S0-mC4d1; 3, S0-mC4d2; 4, mC4d alone. Molecular weight of S0, 26.3 kDa; S0-mC4d1, 68.8 kDa; S0-mC4d2, 110.7 kDa; mC4d alone, 44.6 kDa.

Table 8. Purity levels and pure protein yields for recombinant, target proteins.

	S0	S0-mC4d1	S0-mC4d2	mC4d alone
Purity (%)	100	95	89	98
Yield (mg/500 mL)	---	1.2	0.83	10

Relative purity levels of each target protein were determined by calculating the percentage of the target protein band within the total band volume of the associated SDS-PAGE gel lane. S0 and mC4d samples had high purity, 99% and 98%, respectively. The two fusion proteins also had high levels of purity, S0-mC4d1 was 95% pure and S0-mC4d2 was 89% pure. 1.2 mg of pure S0-mC4d1, 0.83 mg of pure S0-mC4d2, and 10 mg of pure mC4d can be obtained from a 500 mL culture of bacteria. Purity levels and yield information are provided in table 8.

2. *In vivo* immunization for development of PEDV recombinant subunit vaccine

Purified proteins previously collected were used to immunize mice. The detailed scheme and dosages are detailed in the materials and methodology.

1) S0-specific humoral immune response

The humoral immune response in response to target proteins were illuminated through indirect ELISA was performed using the serum of immunized mice. As C4d specific auto-reactive T-helper cells encourage B cells to differentiate and produce antibody, fusion proteins would increase the presence of S0 specific antibody within the serum of C4d-immunized mice. As seen in figure 24A and 24B, anti-S0 IgG titers did not differ between treatment groups representing a lack of an early response to immunization with C4d. However, according to

figure 24C and 24D, treatment groups differentiated at the 4-week mark and further differentiated after 6 weeks. At 4 weeks, S0-mC4d1 and S0-mC4d2 had a significantly higher antibody titers than the untreated group, and the S0 group. These results indicate that the fusion of tandem repeats of mC4d to S0 (S0-mC4d1 and S0-mC4d2) has potential adjuvanticity in terms of generating a humoral immune response against S0 by providing ample amounts of total IgG compared to the S0 group. This means that C4d conjugation increases the adjuvanticity of the S0 subunit vaccine. After 6 weeks the groups continue to remain significantly higher than the untreated PBS group and the S0 group. Interestingly, groups 5 and 6 (the two mixture conditions) also presented with a phenotype of high anti-S0 IgG titer at 4 weeks and at 6 weeks. This means that for mC4d's adjuvant effect is not necessarily due to conjugation with an antigen which implies that there is a possibility that mC4d exerts its adjuvant effect without T cell epitope donation. T cell analysis to confirm this statement was deemed necessarily. In conclusion, after 4 weeks, S0-specific antibody responses from groups injected with S0-mC4d1, S0-mC4d2 or either of the two mixture groups showed elevated S0-specific IgG titers, surpassing that of the untreated group, and the S0 control group.

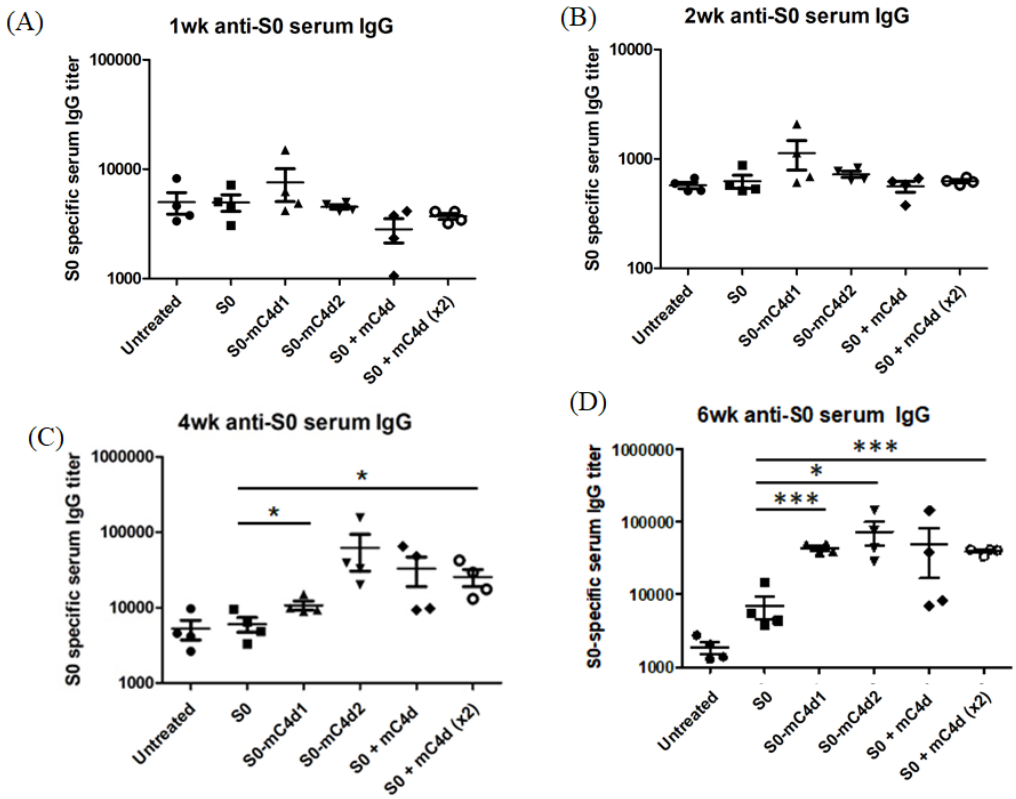

Figure 24 Detection of S0 specific IgG antibodies from mice immunized with S0, S0-mC4d1, S0-mC4d2, S0 + mC4d, or S0 mC4d (x2) subunit vaccines at (A) 7 days, (B) 2 weeks, (C) 4 weeks, and (D) 6 weeks post initial injection. All values represent the means $\pm$ SD (n = 4).

2) S0 and C4d-specific cellular immune response

Due to C4d's theorized mechanism of adjuvanticity, IL-4+ ELISpot assays were used to analyze T cell responses to immunization. T-cells which secreted IL-4 were of interest due to their role in the differentiation of naive T-helper cells into Th2 cells. This course of action usually leads down the humoral immunity route

where Th2 cells assist B cells into producing antibodies (Fiorentino, Bond et al. 1989). Stimulation with S0 or C4d is expected to cause more spots to appear for the fusion and mixture groups if compared with stimulation with plain media or with C3d.

As expected, the untreated group presented with low counts of Th2 cells and also simulation with plain media also resulted in low numbers of Th2 cells in all groups.

The first conclusion that was reached based on the ELISpot data was that fusion proteins generated significant amounts of C4d-specific Th2 cells. As seen in figures 25 and 26, all treatment groups generated a Th2 response when stimulated with S0, this was to be expected. However, as seen in the two groups which were injected with either S0-mC4d1 or S0-mC4d2, the number of spots indicating Th2 cells specific for C4d were significantly higher than all of the other groups, including the S0 group. This indicates that while the S0 group contained Th2 cells specific for S0, S0-mC4d1 and S0-mC4d2 had Th2 cells which specificity for a mixture of both S0 and for mC4d, providing evidence of the existence of complement specific, autoreactive T cells. T cell counts for each individual mouse was plotted on a correlation plot comparing the number of S0-specific and mC4d-specific Th2 cells. The mixed variety of specificity in Th2 cells for S0-mC4d1 and S0-mC4d2 groups can be further validated by viewing the correlation plot shown in figure 27. Light and dark blue dots representing S0-mC4d1 and S0-mC4d2, respectively, have dots toward the line of correlation indicating that they contain

Th2 cells with a balanced amount of S0-specificity and C4d-specificitiy. When viewing the yellow squares, which represent the S0 group, the dots are gathered along the S0-specific axis indicating a bias within that group for only S0-specific Th2 cells. In contrast to the S0 group, S0-mC4d1 and S0-mC4d2 groups T cell counts are dependent, and comprised of, both S0 and mC4d T cells.

Second, through examination of the PBS group, it was apparently that pre-existing, or pre-activated, C4d-specific autoreactive Th2 cells did not exist within this experiment cohort. This can be clearly seen in figure 25 and 26 when viewing specifically the PBS, untreated group. As C4d stimulation did not elicit a spot response within the PBS group, which should not have had prior interactions with C4d, it was concluded that pre-activated C4d-specific Th2 cells responsible for "fast responses" could not be seen at this time and that the C4d-specific Th2 cells were naïve before first encountering C4d during immunization. As mice were only 13 weeks old at the time of sacrifice and were grown in an SPF (specific-pathogen-free) condition, it is plausible that they had not built up enough experiences over a lifetime to generate pre-existing C4d specific Th2 cells. This result also provides a reason for why a fast response failed to show during the measurements of IgG titers at 1 week and 2 weeks post injection.

Lastly, groups 5 and 6, which represent the two mixture regimens, once again presented with an interesting phenotype in response to immunization. S0-specific Th2 was enhanced significantly in contrast with mC4d Th2 cells. Despite being injected with S0 and with C4d, the mixture groups presented with a Th2 phenotype

indicating that low numbers of Th2 cells specific with either S0 or C4d had been activated. In fact, the numbers of C4d-specific Th2 cells in either mixture group were lower than that of the C3d numbers, an unrelated protein, in the S0 group. This demonstrates that the significantly higher IgG response to S0-mC4d1 and S0-mC4d2 are dependent on mC4d-specific Th2 cells. The superior IgG response found in the mixture groups are dependent on mC4d which act through other mechanisms that S0 conjugated to mC4d do not experience.

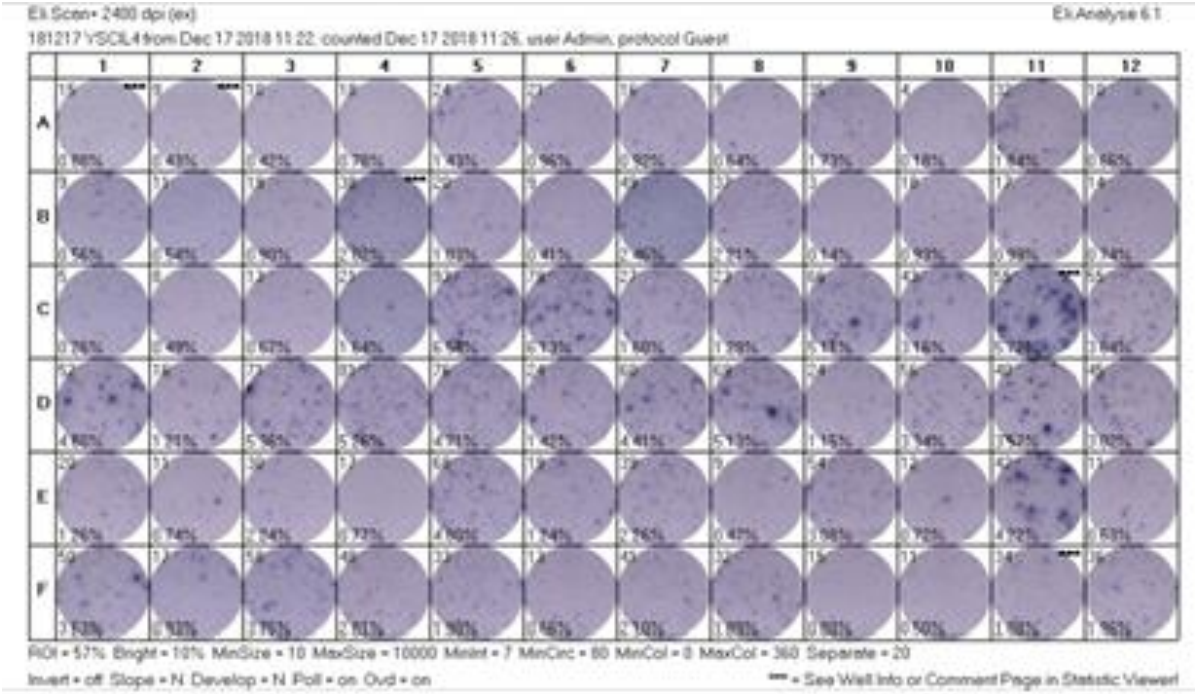

Figure 25. IL-4 secretion in splenocytes through comparison of spots from murine spleen T cells after stimulation with plain media (Rows A and B), S0 (Rows C and D), or C4d (Rows E and F) for IL-4 secretion. Distribution of groups: Untreated group, A1-A4, C1-C4, E1-E4; S0 group, A5-A8, C5-C8, E5-E8; S0-mC4d1, A9-A12, C9-C12, E9-E12; S0-mC4d2, B1-B4, D1-D4, F1-F4; S0 + mC4d, B5-B8, D5-D8, F5-F8; S0 + mC4dx2, B9-B12, D9-D12, F9-F12.

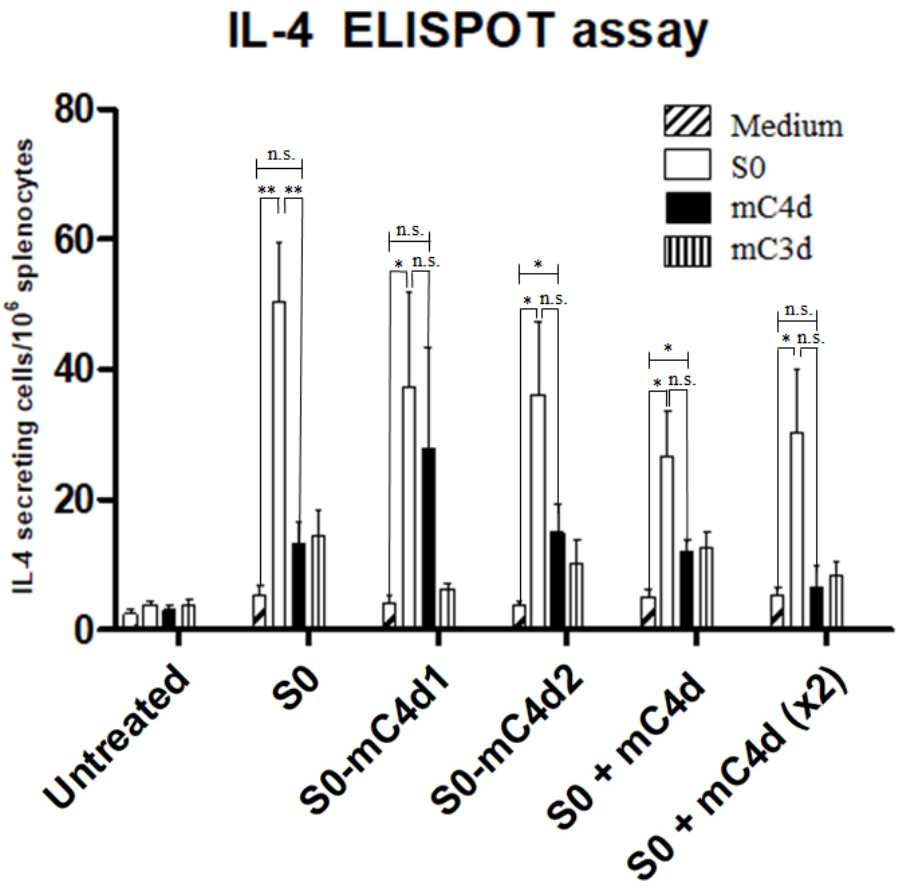

Figure 26 Th2 cell counts determined by T cell release of IL-4 in response to protein stimulation represented by average number of spots in ELISpot assay.

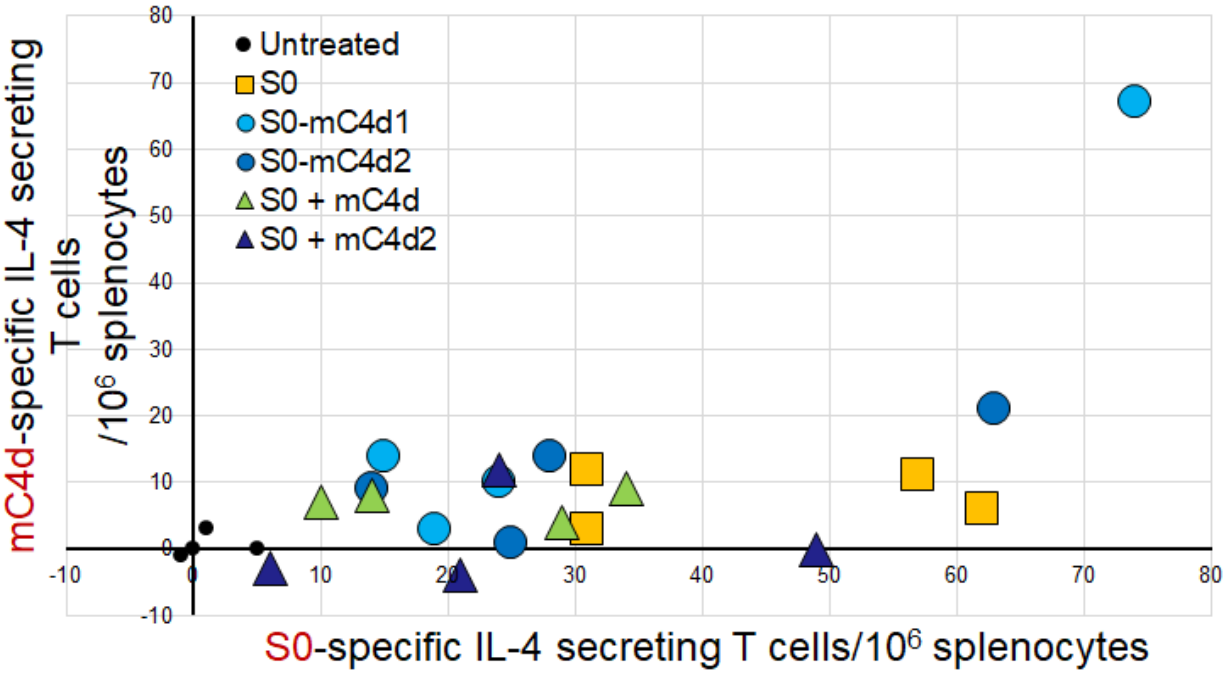

Figure 27. Correlation between mC4d specific IL-4 secreting T cells and S0 specific IL-4 secreting T cells. The x-axis represents counts of S0-specific IL-4 secreting T cells and the y-axis represents mC4d-specific IL-4 secreting T cells. Each dot represents an individual mouse with groups denoted by the symbols shown in the legend.

Overall, according to ELISpot assay results, all treatment groups contained Th2 cells which would produce IL-4 in response to S0 and the fusion adjuvant groups T cells produce IL-4 in response to both S0 and C4d. The existence of pre-activated Th2 cells specific for C4d was unable to be shown in this study. In addition, due to the, surprisingly, low counts of Th2 cells in the two mixture groups, their cause for increased IgG titers cannot be explained using C4d specific T cells. Thus, the conclusion that the IL-4 secretion response to the fused addition of C4d in the subunit vaccine is related with the role of C4d, according to only the ELISpot assay data. Coupled with the end point antibody titer analysis showing that the S0-mC4d1, S0-mC4d2, and, mysteriously, the two mixture groups had higher antibody titer than the S0 control, the suggestion that C4d has a role in bolstering humoral immunity stands.

V. Conclusion

Subunit vaccine production through *E. coli* bioreactor expression systems provides rapid production and upscaling in order to combat PEDV in a fast and powerful manner. While providing benefits to research and the livestock feed additive industries, there yet exists obstacles to overcome such as producing enough amounts of soluble proteins and producing a subunit vaccine with enough immunogenicity to compete with live attenuated vaccines. In order to increase the immunogenicity of the S0 subunit vaccine for PEDV, complement fragment C4d was used as a fusion adjuvant.

For optimization of soluble protein expression, the major finding was that co-expression of the recombinant proteins with *tig* chaperone along with inducing said proteins with IPTG at a set point optical density value that represents the mid-log phase (A_{600} = 0.4 – 0.6) will enhance the solubility of the proteins produced. In this context, this study has some major significance in vaccine development regarding optimization of soluble protein expression and in producing a fusion adjuvant system utilizing C4d.

In vivo immunization and experimentation showed that an S0 specific IgG humoral immune response was found in mice injected with S0-mC4d2 or either of the mixture groups after 4 weeks. Said humoral response even outperformed the subunit vaccine using a powerful laboratory adjuvant. After 6 weeks, end point IgG antibody titers were significantly higher than the PBS or S0 controls in all

treatment groups which contained C4d indicating C4d's prowess as a powerful adjuvant. T cell analysis showed that fusion adjuvant treatment groups responded to C4d stimulation by secreting IL-4 indicating the presence of C4d-specific autoreactive Th2 cells. Interestingly, although the two mixture regimens produced high end point IgG titer, the production of said antibody appears to be unrelated to the presence of Th2 cells specific to C4d. Based on the results, the fusion adjuvant C4d or C4d vaccine cocktail may be a promising new adjuvant combination utilized in PEDV vaccines in the future.

Works Cited

Ayudhya, S. N. N., P. Assavacheep, R. J. T. Thanawongnuwech and e. diseases (2012). "One World–One Health: the threat of emerging swine diseases. an Asian perspective." **59**: 9-17.

Burnette, W. N. J. C. o. i. b. (1991). "Recombinant subunit vaccines." **2**(6): 882-892.

Carroll, M. C. J. V. (2008). "Complement and humoral immunity." **26**: I28-I33.

Coller, B.-A. G., D. E. Clements, A. J. Bett, S. L. Sagar and J. H. J. V. Ter Meulen (2011). "The development of recombinant subunit envelope-based vaccines to protect against dengue virus induced disease." **29**(42): 7267-7275.

Crooke, E., B. Guthrie, S. Lecker, R. Lill and W. J. C. Wickner (1988). "ProOmpA is stabilized for membrane translocation by either purified E. coli trigger factor or canine signal recognition particle." **54**(7): 1003-1011.

Crowe, J., B. S. Masone and J. J. M. b. Ribbe (1995). "One-step purification of recombinant proteins with the 6xHis tag and Ni-NTA resin." **4**(3): 247-258.

Cuadros, C., F. J. Lopez-Hernandez, A. L. Dominguez, M. McClelland, J. J. I. Lustgarten and immunity (2004). "Flagellin fusion proteins as adjuvants or vaccines induce specific immune responses." **72**(5): 2810-2816.

De Groot, A. S., T. M. Ross, L. Levitz, T. J. Messitt, R. Tassone, C. M. Boyle, A. J. Vincelli, L. Moise, W. Martin, P. M. J. I. Knopf and c. biology (2015). "C3d adjuvant effects are mediated through the activation of C3d- specific autoreactive T cells." **93**(2): 189-197.

Fahnert, B., H. Lilie and P. Neubauer (2004). Inclusion bodies: formation and utilisation. Physiological Stress Responses in Bioprocesses, Springer**:** 93-142.

Falsey, A. R. and E. E. J. V. Walsh (1997). "Safety and immunogenicity of a respiratory syncytial virus subunit vaccine (PFP-2) in the institutionalized elderly." **15**(10): 1130-1132.

Feucht, H. E. J. A. J. o. T. (2003). "Complement C4d in graft capillaries–the missing link in the recognition of humoral alloreactivity." **3**(6): 646-652.

Fiorentino, D. F., M. W. Bond and T. J. J. o. E. M. Mosmann (1989). "Two types of mouse T helper cell. IV. Th2 clones secrete a factor that inhibits cytokine production by Th1 clones." **170**(6): 2081-2095.

Galloway, C. A., M. P. Sowden and H. C. J. B. Smith (2003). "Increasing the yield of soluble recombinant protein expressed in E. coli by induction during late log phase." **34**(3): 524-530.

Gershon, R. K. (1974). T cell control of antibody production. Contemporary topics in immunobiology, Springer**:** 1-40.

Herzenberg, A. M., J. S. Gill, O. Djurdjev and A. B. J. J. o. t. A. S. o. N. Magil (2002). "C4d deposition in acute rejection: an independent long-term prognostic factor." **13**(1): 234-241.

Hoffmann, A., B. Bukau and G. J. B. e. B. A.-M. C. R. Kramer (2010). "Structure and function of the molecular chaperone Trigger Factor." **1803**(6): 650-661.

Huang, Y.-W., A. W. Dickerman, P. Piñeyro, L. Li, L. Fang, R. Kiehne, T. Opriessnig and X.-J. J. M. Meng (2013). "Origin, evolution, and genotyping of emergent porcine epidemic diarrhea virus strains in the United States." **4**(5): e00737-00713.

Huleatt, J. W., V. Nakaar, P. Desai, Y. Huang, D. Hewitt, A. Jacobs, J. Tang, W. McDonald, L. Song and R. K. J. V. Evans (2008). "Potent immunogenicity and

efficacy of a universal influenza vaccine candidate comprising a recombinant fusion protein linking influenza M2e to the TLR5 ligand flagellin." **26**(2): 201-214.

Janeway, C. A. (1989). Approaching the asymptote? Evolution and revolution in immunology. Cold Spring Harbor symposia on quantitative biology, Cold Spring Harbor Laboratory Press.

Janeway, C. A., P. Travers, M. Walport and M. J. Shlomchik (2005). "Immunobiology: the immune system in health and disease."

Jarvis, M. C., H. C. Lam, Y. Zhang, L. Wang, R. A. Hesse, B. M. Hause, A. Vlasova, Q. Wang, J. Zhang and M. I. J. P. v. m. Nelson (2016). "Genomic and evolutionary inferences between American and global strains of porcine epidemic diarrhea virus." **123**: 175-184.

Kang, T.-J., Y.-S. Kim, Y.-S. Jang and M.-S. J. V. Yang (2005). "Expression of the synthetic neutralizing epitope gene of porcine epidemic diarrhea virus in tobacco plants without nicotine." **23**(17-18): 2294-2297.

Kaur, J., A. Kumar and J. J. I. j. o. b. m. Kaur (2018). "Strategies for optimization of heterologous protein expression in E. coli: Roadblocks and reinforcements." **106**: 803-822.

Kim, H., Y.-k. Lee, S. C. Kang, B. K. Han, K. M. J. C. Choi and e. v. research (2016). "Recent vaccine technology in industrial animals." **5**(1): 12-18.

KUSANAGI, K.-i., H. KUWAHARA, T. KATOH, T. NUNOYA, Y. ISHIKAWA, T. SAMEJIMA and M. J. J. o. V. M. S. TAJIMA (1992). "Isolation and serial propagation of porcine epidemic diarrhea virus in cell cultures and partial characterization of the isolate." **54**(2): 313-318.

Lee, C. J. V. j. (2015). "Porcine epidemic diarrhea virus: an emerging and re-emerging epizootic swine virus." **12**(1): 193.

Lee, S. and C. J. E. i. d. Lee (2014). "Outbreak-related porcine epidemic diarrhea virus strains similar to US strains, South Korea, 2013." **20**(7): 1223.

Lee, S. E., S. Y. Kim, B. C. Jeong, Y. R. Kim, S. J. Bae, O. S. Ahn, J.-J. Lee, H.-C. Song, J. M. Kim, H. E. J. I. Choy and immunity (2006). "A bacterial flagellin, Vibrio vulnificus FlaB, has a strong mucosal adjuvant activity to induce protective immunity." **74**(1): 694-702.

Li, C., W. Li, E. L. de Esesarte, H. Guo, P. van den Elzen, E. Aarts, E. van den Born, P. J. Rottier and B.-J. J. J. o. v. Bosch (2017). "Cell attachment domains of the PEDV spike protein are key targets of neutralizing antibodies." JVI. 00273-00217.

Lilie, H., E. Schwarz and R. J. C. o. i. b. Rudolph (1998). "Advances in refolding of proteins produced in E. coli." **9**(5): 497-501.

Lin, C.-N., W.-B. Chung, S.-W. Chang, C.-C. Wen, H. Liu, C.-H. Chien and M.-T. J. J. o. V. M. S. Chiou (2014). "US-like strain of porcine epidemic diarrhea virus outbreaks in Taiwan, 2013–2014." **76**(9): 1297-1299.

Masuda, T., S. Murakami, O. Takahashi, A. Miyazaki, S. Ohashi, H. Yamasato and T. J. A. o. v. Suzuki (2015). "New porcine epidemic diarrhoea virus variant with a large deletion in the spike gene identified in domestic pigs." **160**(10): 2565-2568.

Murata, K. and W. M. J. T. R. Baldwin III (2009). "Mechanisms of complement activation, C4d deposition, and their contribution to the pathogenesis of antibody-mediated rejection." **23**(3): 139-150.

Nam, E. and C. J. V. m. Lee (2010). "Contribution of the porcine aminopeptidase N (CD13) receptor density to porcine epidemic diarrhea virus infection." **144**(1-2): 41-50.

Nickeleit, V., M. Zeiler, F. Gudat, G. Thiel and M. J. J. o. t. A. S. o. N. Mihatsch (2002). "Detection of the complement degradation product C4d in renal allografts: diagnostic and therapeutic implications." **13**(1): 242-251.

O'Hagan, D. T. and E. J. D. d. t. De Gregorio (2009). "The path to a successful vaccine adjuvant–'the long and winding road'." **14**(11-12): 541-551.

Oh, J., K.-W. Lee, H.-W. Choi and C. J. A. o. v. Lee (2014). "Immunogenicity and protective efficacy of recombinant S1 domain of the porcine epidemic diarrhea virus spike protein." **159**(11): 2977-2987.

Oh, J. S., D. S. Song and B. K. J. J. o. v. s. Park (2003). "Identification of a putative cellular receptor 150 kDa polypeptide for porcine epidemic diarrhea virus in porcine enterocytes." **4**(3): 269-275.

Perrie, Y., D. Kirby, V. W. Bramwell, A. R. J. R. p. o. d. d. Mohammed and formulation (2007). "Recent developments in particulate-based vaccines." **1**(2): 117-129.

Perrie, Y., A. R. Mohammed, D. J. Kirby, S. E. McNeil and V. W. J. I. j. o. p. Bramwell (2008). "Vaccine adjuvant systems: enhancing the efficacy of sub-unit protein antigens." **364**(2): 272-280.

Piao, D.-C., Y.-S. Lee, J.-D. Bok, C.-S. Cho, Z.-S. Hong, S.-K. Kang, Y.-J. J. P. e. Choi and purification (2016). "Production of soluble truncated spike protein of porcine epidemic diarrhea virus from inclusion bodies of Escherichia coli through refolding." **126**: 77-83.

Platt, J. L. J. J. o. t. A. S. o. N. (2002). "C4d and the fate of organ allografts." **13**(9): 2417-2419.

Reed, S. G., M. T. Orr and C. B. J. N. m. Fox (2013). "Key roles of adjuvants in modern vaccines." **19**(12): 1597.

Schein, C. H. J. N. B. (1989). "Production of soluble recombinant proteins in bacteria." **7**(11): 1141.

Singh, S. M., A. K. J. J. o. b. Panda and bioengineering (2005). "Solubilization and refolding of bacterial inclusion body proteins." **99**(4): 303-310.

Song, D., H. Moon, B. J. C. Kang and e. v. research (2015). "Porcine epidemic diarrhea: a review of current epidemiology and available vaccines." **4**(2): 166-176.

Song, D. and B. J. V. g. Park (2012). "Porcine epidemic diarrhoea virus: a comprehensive review of molecular epidemiology, diagnosis, and vaccines." **44**(2): 167-175.

Sørensen, H. P. and K. K. J. M. c. f. Mortensen (2005). "Soluble expression of recombinant proteins in the cytoplasm of Escherichia coli." **4**(1): 1.

Starr, T. K., S. C. Jameson and K. A. J. A. r. o. i. Hogquist (2003). "Positive and negative selection of T cells." **21**(1): 139-176.

Sun, R.-Q., R.-J. Cai, Y.-Q. Chen, P.-S. Liang, D.-K. Chen and C.-X. J. E. i. d. Song (2012). "Outbreak of porcine epidemic diarrhea in suckling piglets, China." **18**(1): 161.

Suo, S., Y. Ren, G. Li, D. Zarlenga, R.-e. Bu, D. Su, X. Li, P. Li, F. Meng and C. J. V. r. Wang (2012). "Immune responses induced by DNA vaccines bearing Spike gene of PEDV combined with porcine IL-18." **167**(2): 259-266.

Tristram, D., R. Welliver, C. Mohar, D. Hogerman, S. Hildreth and P. J. J. o. I. D. Paradiso (1993). "Immunogenicity and safety of respiratory syncytial virus subunit vaccine in seropositive children 18-36 months old." **167**(1): 191-195.

Wang, E., D. Guo, C. Li, S. Wei, Z. Wang, Q. Liu, B. Zhang, F. Kong, L. Feng and D. J. P. o. Sun (2016). "Molecular characterization of the ORF3 and S1 Genes of porcine epidemic diarrhea virus non S-INDEL strains in seven regions of China, 2015." **11**(8): e0160561.

Summary in Korean

돼지유행성설사병 바이러스의 외피단백질 일부분인 S0 아단위 백신의 면역원성을 높이기 위해서, 보체 절편인 C4d가 결합형 어쥬번트로 이용되었다.

S0, S0−mC4d1, S0−mC4d2, mC4d를 E. coli 발현 벡터에 성공적으로 클로닝하였다. 각 벡터의 시퀀스는 Sanger 시퀀싱과 제한효소 소화 후 전기영동 확인방법을 통해 확인하였다. 그 이후, 단백질을 soluble하게 발현하는 것이 중요하므로 3 가지 요소를 통해 solubility를 증진시키고자 하였다. 첫 번째 방법은 샤페론 단백질의 도입이고, 두 번째 방법은 최적의 단백질 유도 optical density를 확인하는 것이며, 세 번째 방법은 단백질 유도 최적의 IPTG 농도를 찾는 것이다. 연구를 통해 샤페론의 발현이 soluble 단백질 발현에 필수적임을 알았고, 최적의 조건이 optical density 0.6, IPTG 0.1 mM임을 확인하였다. 이렇게 확인한 조건으로 S0, S0−mC4d1, S0−mC4d2, mC4d 단백질은 500 ml scale로 생산되어 정제, 투석, 농축 과정을 거쳐 동물실험에 사용되었다. 6 그룹의 마우스에 동일 몰의 단백질을 투여한 후 mC4d의 어쥬번트 효과를 보았다. 그룹은 PBS 음성 대조구, S0, S0−mC4d1, S0−mC4d2, S0와 mC4d 혼합물, S0와 mC4d 2배의 혼합물이었다. 면역접종 후 2,4,6 주 후에 혈청을 통해 S0 특이적 IgG를 분석했고, 6주에 비장을 분리하여 T 세포 분석을 하였다. 그 결과 mC4d를 결합 그룹은 S0 그룹에 비해 S0 특이적 IgG가 유의적으로 많았으며, mC4d 혼합물 그룹 역시 다량의 S0 특이적 IgG를 생산했다. IL−4 ELISpot 분석을

통해 비장 T 세포를 분석한 결과 mC4d 결합의 경우 mC4d 특이적 T 세포가 어쥬번트 역할의 원인이 된 것으로 파악된다.

결론적으로, mC4d 결합형 단백질은 높은 purity와 S0에 대한 높은 면역원성을 가지며, mC4d 혼합물 역시 높은 면역원성을 기록함으로써 어쥬번트 활용의 가치가 있음을 확인했다.

주요어: 돼지유행성설사병, 돼지유행성설사병 바이러스, 어쥬번트, 아단위 백신, 보체 절편, C4d, 결합형 어쥬번트, 외피단백질, 재조합 단백질, 최적화, solubility

학번: 2016-27810

Acknowledgement

이 졸업논문을 일년 전 돌아가신 저의 할머님(조순예)께 바칩니다. 제 인생에 늘 함께 하시고 저의 성장에 수고를 아끼지 않으시며, 항상 따뜻한 마음으로 배려해 주신 분. 그립습니다.

먼저 최윤재 교수님께 감사드립니다. 그리고, 강상기 교수님, 조종수 교수님, 동물 세포 공학 연구실의 멋진 구성원 선배님들과 후배들. 지난 3 년 동안 짧다고 느껴졌을 지 몰라도 엄청나게 많은 학습과 좋은 추억을 간직하게 된 실험실. 인내와 이해, 그리고 저를 성공적으로 마무리 하도록 열정적으로 도와 주심에 감사드립니다. 이 프로젝트의 완성과 졸업은 교수님들과 실험실 모든 분들의 도움 없이는 불가능했습니다.

먼저 진심으로 감사드립니다.

지도 교수 – 최윤재 교수님.

저의 잠재력을 발견하시고 저를 선택해 공부할 수 있는 기회를 주셔서 감사합니다. 저는 교수님께 열심히 공부하며 많은 것을 배우고 여러 방면으로 사회인으로 성장하였습니다. 교수님의 가르침으로 저의 인생에 많은 도움이 되리라 생각합니다.

강상기 교수님, 비록 실험실 모임에서 만날 수 있었지만 많은 도움을 주셔서 감사합니다. 특히 처음에는 연구 나 발표에 관해 미숙한 저에게 항상 명확하게 조언해 주시고 그로 인해 연구원으로서 저의 기술이 많이 향상되었습니다. 멘토로서, 교수님의 도움은 정말 귀중한 것이며, 제 인생의 영향력 있는 교사로 기억할 것입니다.

조종수 교수님, 실험실 모임에서 저에게 조언 해 주신 것에 감사드립니다. 연구에 대한 열정과 새로운 것을 배우는 것에 대해서도 흥미를 가질 수 있었습니다.

윤철희 교수님, 저의 질문과 변론을 들어 주셔서 감사합니다. 교수님의 질문에 대답 할 수 있도록 연구하며 공부하고 지난 5 학기 동안 배운 것에 대한 지식을 총 동원하여 발표함으로서 석사 학위를 잘 준비 하게 되었습니다. 또한, 교수님의 배려 깊은 친절 함으로 인하여 저의 능력에 대한 자신감을 갖게 되었습니다. 저를 믿어 줘서 고맙습니다.

저를 잘 돌봐 주시고 학업에 열심히 하도록 도와 주신 가족들.

큰 외삼촌 영호 삼촌 과 그의 아내 숙모님! 이 실험실을 알게 해 주시고 저를 사랑스러운 딸처럼 대하며 졸업 할 수 있도록 배려와 조언 해 주셔서 감사합니다. 3 년 동안 저를 믿고 기다려 주셔 감사

합니다. 준겸 오빠, 유겸 오빠, 그리고 희겸 오빠. 오빠들은 모든 것이 낯선 이곳에서 확실히 사촌 오빠들이었습니다. 슬프다고 느낄 때 맛있는 저녁 식사를 사거나 영화를 보여 주고 외롭지 않도록 도와 주었어요. 함께 많은 시간을 보내며 즐거웠습니다. 특히 희겸오빠!

학교생활에서도 많은 도움 주고 같은 학교에 다니는 사촌오빠가 있어 얼마나 많은 도움이 되던지 알려준 오빠 고마워요.

그리고 더 없이 고마운 이모 와 이모부!!!

갈 곳 없는 저에게 아무것 바라지 않으며 편안하게 공부할 수 있도록 집에 머물게 해 주시고 자신들의 아이처럼 저를 돌보아 주셔 제 집처럼 아무 불편함 없이 기쁘게 지냅니다. 어려운 일이 있을때마다 항상 귀찮다 안 하고 해결해 주시고 진심으로 감사합니다. 이모와 이모부의 도움없이 할 수 없었습니다. 미나언니, 당신이 항상 저에게 친절했기 때문에 함께 시간을 보내고 음식을 먹는 것이 정말 행복했습니다. 나는 우리가 함께 많은 시간을 보낼 수 있기를 바랍니다. 또한 영삼삼촌! 함께 시간을 보내고 친절하게 대해 주셔서 감사합니다.

학교 생활이 힘들었지만 온 가족들의 배려와 지원이 있었기 때문에 포기하지 않고 지금의 이 자리 가능했습니다.

소중한 부모님에게는 단순한 말로 감사 표현를 다 할 수 없습니다. 성공과 멋진 일을 할 수 있도록 저를 낳아 주셔서 감사합니다. 그동안 부모님은 제가 하고 싶었던 결정들을 지지했습니다. 일이 생길때마다, 나에게 모두 옳은 말을 하고 그것은 포기하지 않고 힘든 고난을 겪어 보다 큰 일을 성취 할 수 있는 힘과 용기를 주었습니다. 언제나 내 편이 되어 주고 격려를 아끼지 않는 마음 늘 감사 할뿐입니다. 정말로, 이 세상에서 내가 가진 유일한 사람들은 엄마입니다. 그리고 아빠.

For Young-Woen, my “forever” my little brother, I hope that when I come back, we can make up for the lost time. Just as you lifted my spirits, I wish to do the same for you. Here is to many more years of me forcing you to pass the difficult game levels for me, bringing coffee home, and driving me to the grocery store. I know that you will always hunger for justice (with a side of spaghetti)! Even though I was so far away for a long time, I didn’t forget about my relatives in the US who supported me from a distance. To especially Michelle, Susan, Joey 삼촌, and Cindy who always gave me great advice and comfort, I could always rely on you all for cheering up and reminding me that I have a home to return to. Don’t worry, I promise to return with the black mamba. To all of my friends who helped me, whether in Korea, as fellow foreigners, or back in the States, thank you for telling me that I could do the impossible. Especially you, Maggie, thank you so much for knowing when I needed you the most.

실험실은 여러 해가 지나면서 저는 훌륭한 선.후배님들과 함께 있을 수 있는 행운을 가졌습니다. 이미 졸업 한 선배님들! 준영 오빠, 호빈 오빠, 인선 언니, 건구 오빠, 수나 언니, 소연 언니, 어진 언니, 재연 언니, 수빈 언니, 과학, 실험실 작업 및 다른 사람들! 일하는 것에 대해 가르쳐 주셔 감사합니다. 우리가 함께 보낸 시간은 정말 재미 있었고 즐겁고 기뻤으며 모두 훌륭한 선배였습니다. 똑똑한 준영에게 오빠, 제가 신입생이었을 때, 저에게 많은 것을 가르쳐 주었고 비록 오빠는 mealworms 에 대해 아무것도 몰랐지만, 여전히 저를 도와주며 한국인을 잘 이해 할 수 없는 것에 공감도 해 주셨죠. 호빈 오빠, 너무 재미 있는 오빠. 인생이 항상 그렇게 심각하지 않다는 것을 상기시켜 주셔서 감사합니다. 인선 언니, 비록 많은 시간을 보낼 수는 없지만, 친절한 언니이고 훌륭한 연구원 이라고 생각 합니다. 소연 언니, 신입생이었을 때 이미 졸업 했었지만 함께 짧은 시간에 같은 실험실에서 함께하는 것이 좋았습니다. 어진 언니, 신입생이었을 때 언니가 너무 바빠 많은 시간 함께 하지는 못했으나 저를 위해 선배로서 이것저것 이야기해 주시고 감사합니다. 재윤 언니, 서울에서 함께 놀아 주고 참 재미있었습니다. 수빈 언니, 제가 이 실험실에서 처음 왔을 때 금방 엄마처럼 저를 돌보았습니다. 그런 친절 함과 제가 필요로 했던 모든 것을 놀라울 정도로 알고 챙겨 주셔서 저 또한 후배들에게 언니처럼 되기 위해 최선을 다하기로

결심했습니다. 제가 떠난 후에라도 선후배들에게 그렇게 기억 되길 빕니다. 서호 오빠, 제가 논문을 바꿔야했기 때문에 곤경에 처했을 때, 저를 도와 주시고 바쁜 일정에도 불구하고 저에게 많은 실험과 면역학에 대해 많은 것을 가르쳐 주셨고 모든 질문에 대해 참을성 있게 대답했습니다. 너무나도 훌륭한 선배님을 함께 할 수 있어서 정말 행운이고 진심으로 감사합니다. 덕분에 많은 것을 배우고 자랑스럽게 졸업 할 수 있게 되었습니다. 다음 학기에 졸업하시고 원하시는 모든 일 이루시길를 바랍니다. 김휘수 박사님, 졸업 축하합니다! 실험실에서 가장 의지하며 신뢰하는 분으로 제게 베풀어 주신 모든 배려와 도움 무슨 말로 감사드려야 할 지 모르겠습니다. 제가 인턴이었을 때부터 친절하고 배려해 주셔서 감사합니다. 후에 기회가 되시면 좋아 하시는 많은 개와 고양이들과 함께 행복한 삶을 누릴 수 있기를 바랍니다. 이상목(씨?) 오빠, 자신의 방식으로 저를 도우려고 열심히 노력했고, 긍정적인 태도는 또한 열심히 공부하고, 열심히 운동하게 만듭니다. 홍량(아치) 오빠, 정말 밝게 빛나는 것처럼 태어나 낙천적으로 나를 웃게 하고, 중국어로 나쁜 말을 가르쳐 주셔서 감사합니다. 기준 오빠, 친절하고 따뜻하게 잘 대해 주셔 실험실에서 함께 하는 동안 감사했습니다. 마지막 우리 귀여운 우릉이! 후배 보다는 여동생이라는 생각이 드는 친구. 우리가 만나서 좋은 친구가 되어 매우 기쁩니다. 삶에 대한 신선하고 행복한 전망은

저에게 큰 영향을 주었고 저에게 많은 희망을 안겨주었습니다. 당신이 도착했을 때, 나는 많은 재미를 실험실에 가지고 있었습니다! 어쩌면 시간이 지남에 따라 실험실 생활이 어려워 질 수도 있지만, 당신이 할 수 있음을 알고 있습니다. 응원합니다.

S.S., as the one person who is always my number one fan, thanks for supporting me through blood, sweat, and tears. When I felt like it was all over, you were always there for me. Thank you, Otter.

2019년 1월, 관악에서

조영생 올림